# AO System Design for Vision Science

**Donald T. Miller**

Indiana University School of Optometry

CfAO

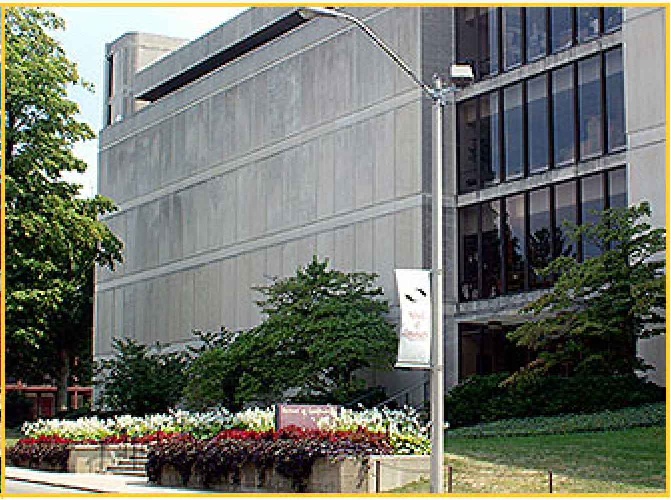

WILEY

# Adaptive Optics for Vision Science

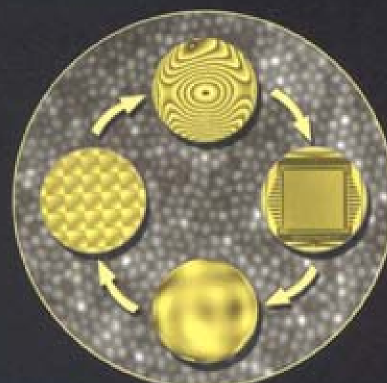

EDITED BY

JASON PORTER,
HOPE QUEENER, JULIANNA LIN,
KAREN THORN, and ABDUL AWWAL

*Wiley Series in Microwave and Optical Engineering • Kai Chang, Series Editor*

# Motivation for High-Resolution Retinal Imaging

1. **Vision begins at the level of the cell.**
   - **Light collecting properties**
   - **Development of the normal eye.**

     (Track retinal processes that vary over time.)
   - **Functionality of the various retinal layers.**

2. **Pathogenesis begins at the level of the cell.**
   - **More precise and timely diagnosis**
   - **More effective monitoring**
   - **Better informed treatment**

# Cell Populations

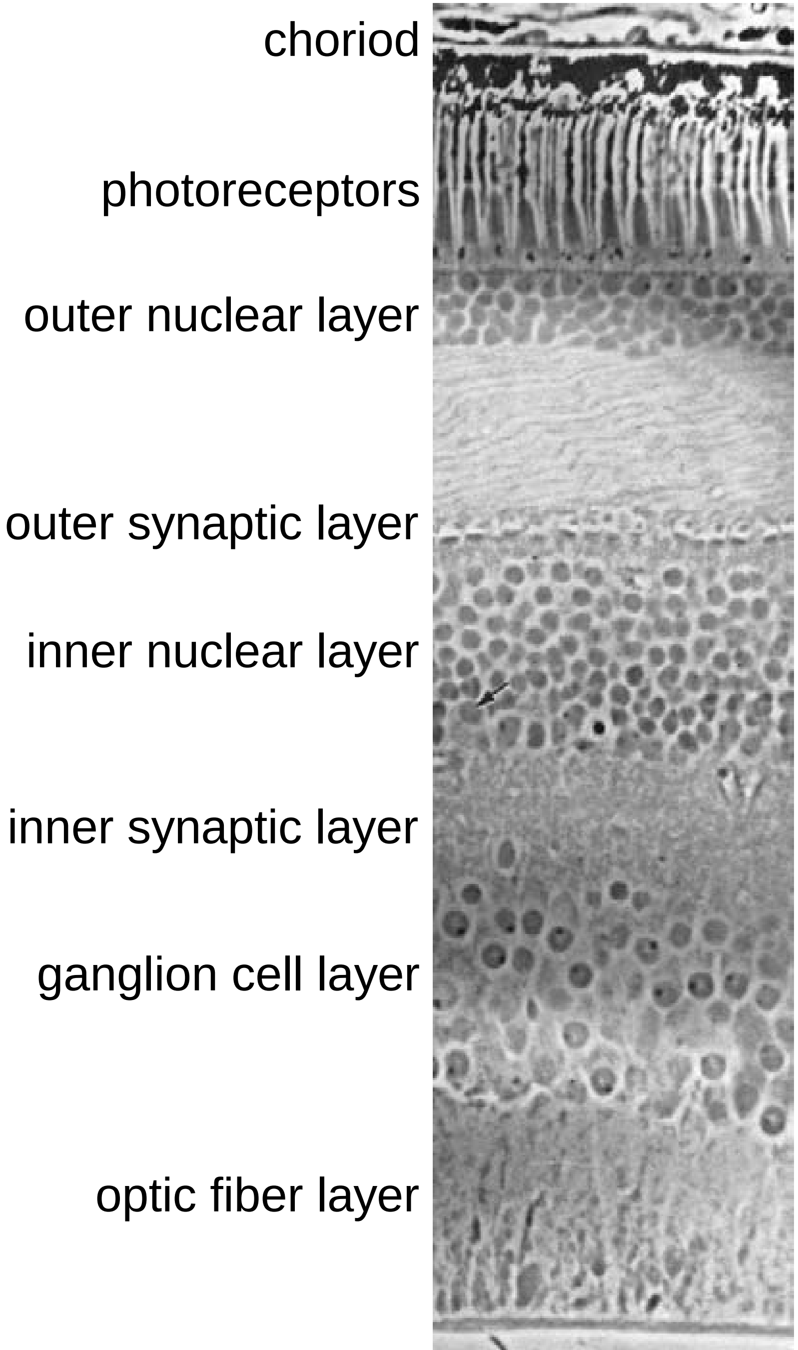


**5 million pigment epithelium**

**6 million cones**
**117 million rods**

100 μm

**? million bipolar**
**? million amacrine**
**? million horizontal**
**? million Muller**

**What cells can we see?**

**1 million ganglion**

**1 million nerve fibers**

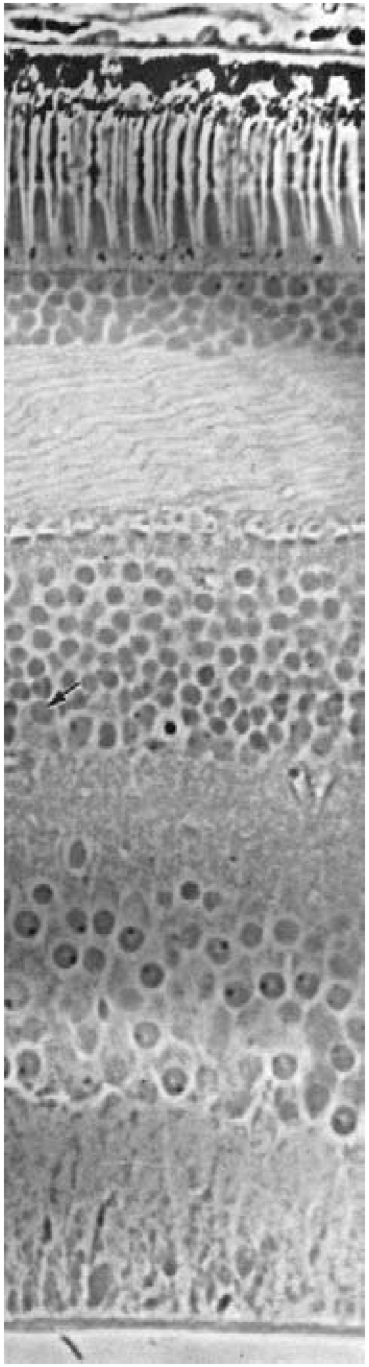

# Camera parameters important for imaging single cells in the living human retina

1. Lateral resolution
2. Axial resolution
3. Exposure time
4. Sensitivity
5. Contrast enhancement

# Point Spread Function vs. Pupil Size

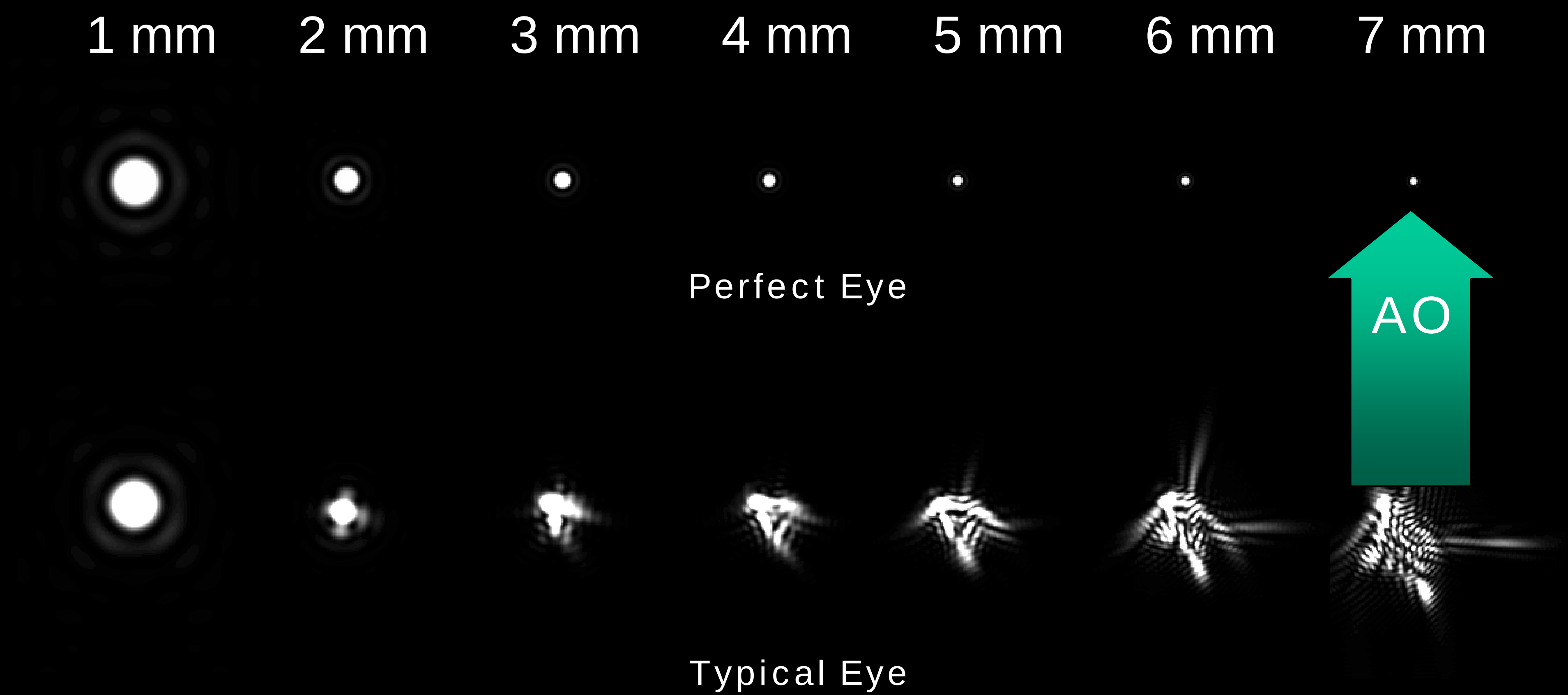


Courtesy A. Roorda

# Aberrations of the eye limit access to high contrast and high spatial frequencies.

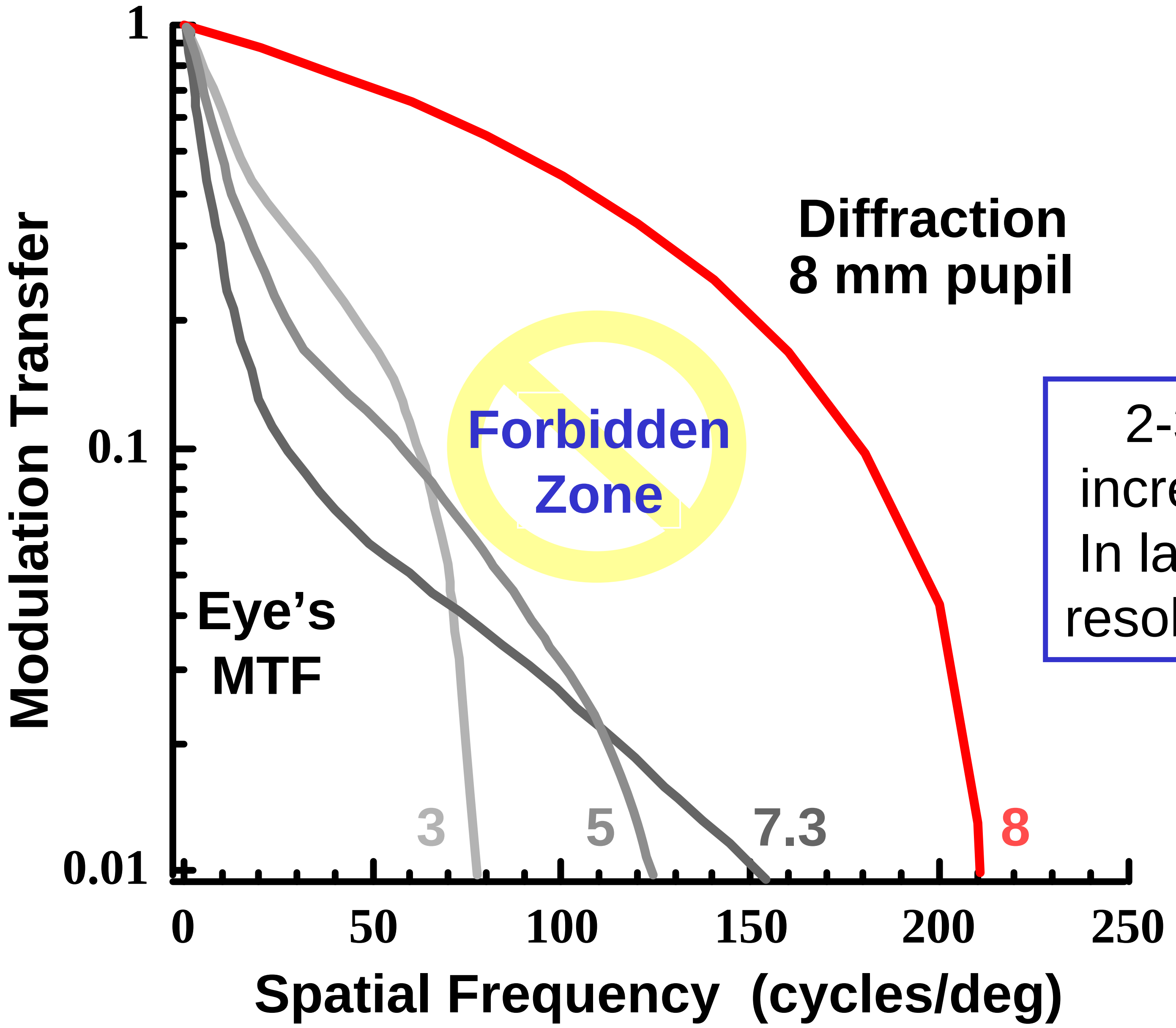


2-3X increase In lateral resolution

# Aberration correction across a large pupil substantially increases the contrast and spatial detail of single cells in the retina.

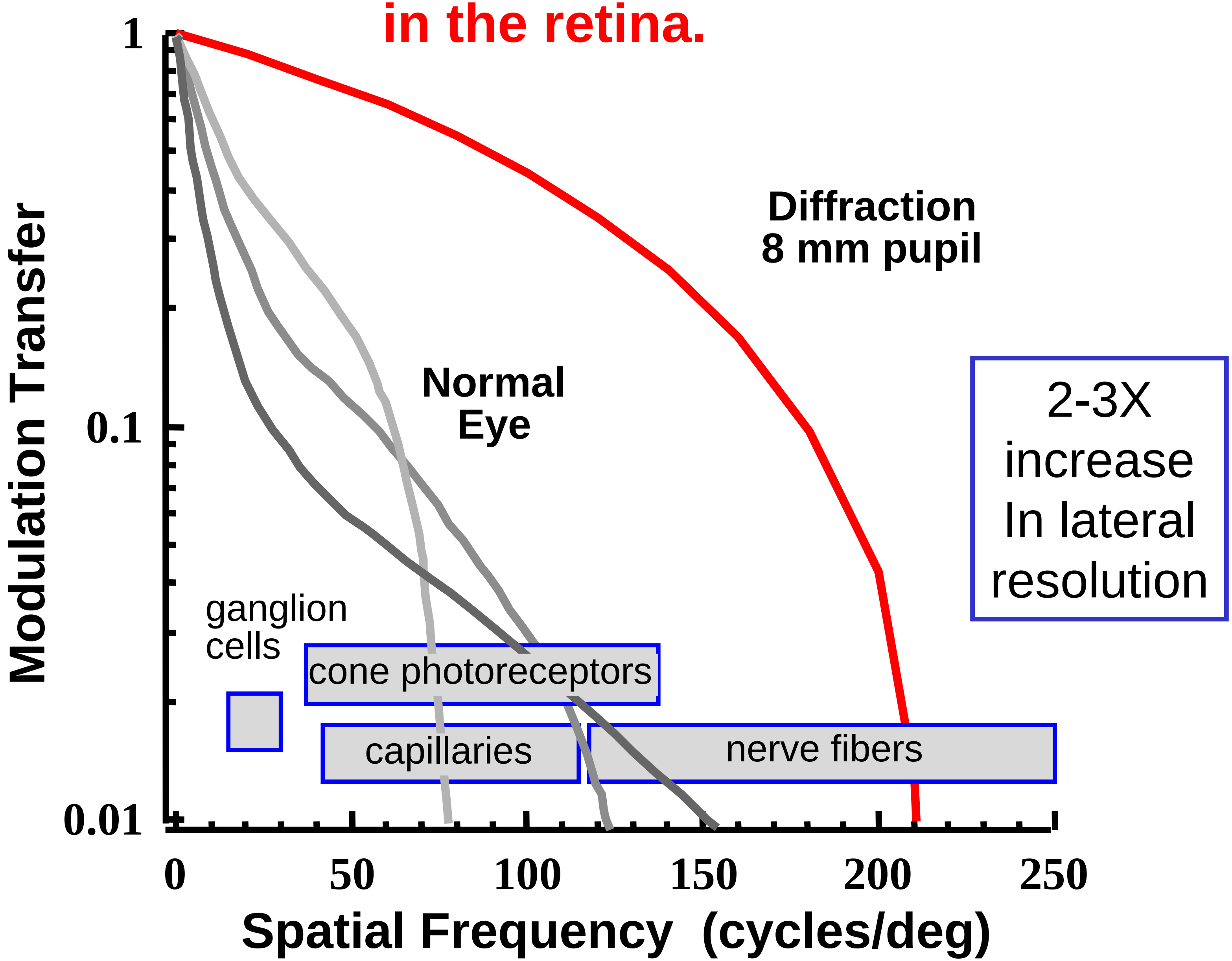

# Adaptive Optics In Astronomy:

-Proposed in 1953 (Horace Babcock)

-First Implemented in mid-1970s

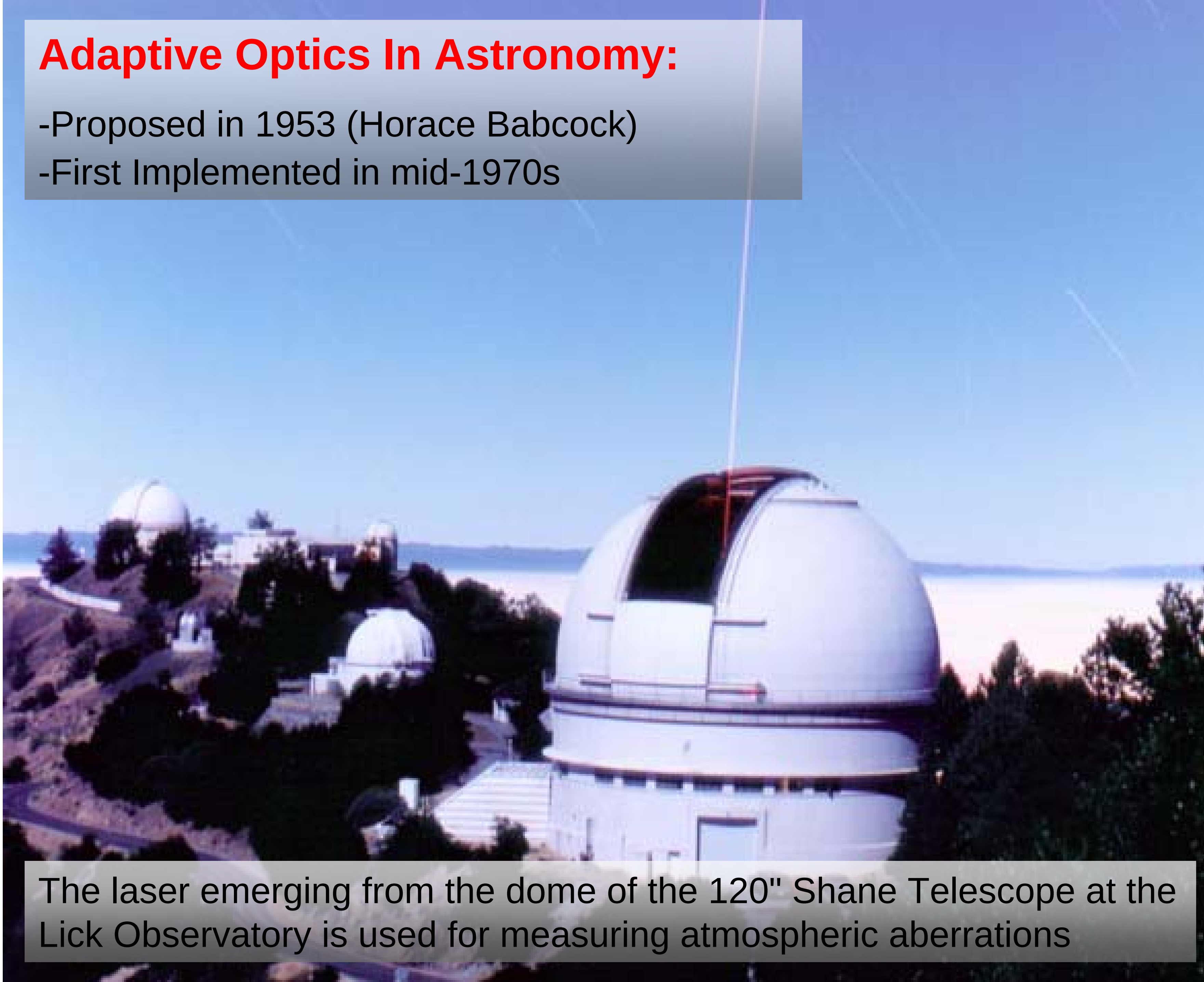

The laser emerging from the dome of the 120" Shane Telescope at the Lick Observatory is used for measuring atmospheric aberrations

# First Use of a Deformable Mirror In the Eye:

A. W.Dreher, J. F. Bille, R. N. Weinreb, "Active optical depth resolution improvement of the laser tomographic scanner," Appl. Opt. **24**, 804-808 (1989).

First use of wavefront sensing to correct higher order aberrations

First demonstration of retinal imaging and vision improvement by correcting higher order aberrations

J. Liang, D.R. Williams, and D.T. Miller, “Supernormal vision and high resolution retinal imaging through adaptive optics,” J. Opt.Soc. Am. A., 14, 2884-2892 (1997).

First AO images on a cone dystrophy patient. Demonstrated that the mosaic was patchy due to photoreceptor dropout

A. Roorda, “Adaptive optics ophthalmoscopy,” *J Ref Surgery*. 2000;16:S602-607.

# Adaptive optics measures and corrects the wave aberrations of the eye

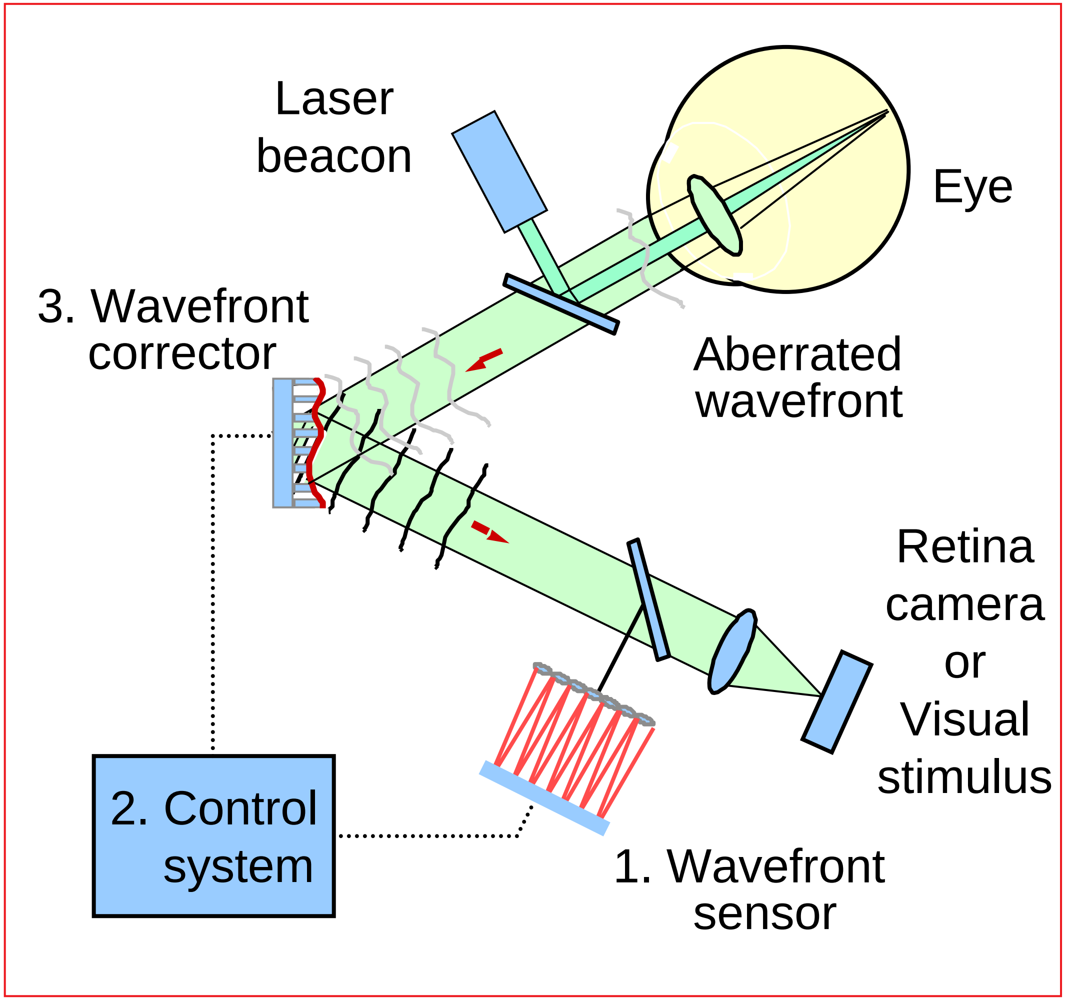


- Permits large pupil (diffraction & NA)
- increased lateral resolution
- Increased collection efficiency of reflected light
- increased axial resolution (SLO)

# Flood-illuminated AO retina camera

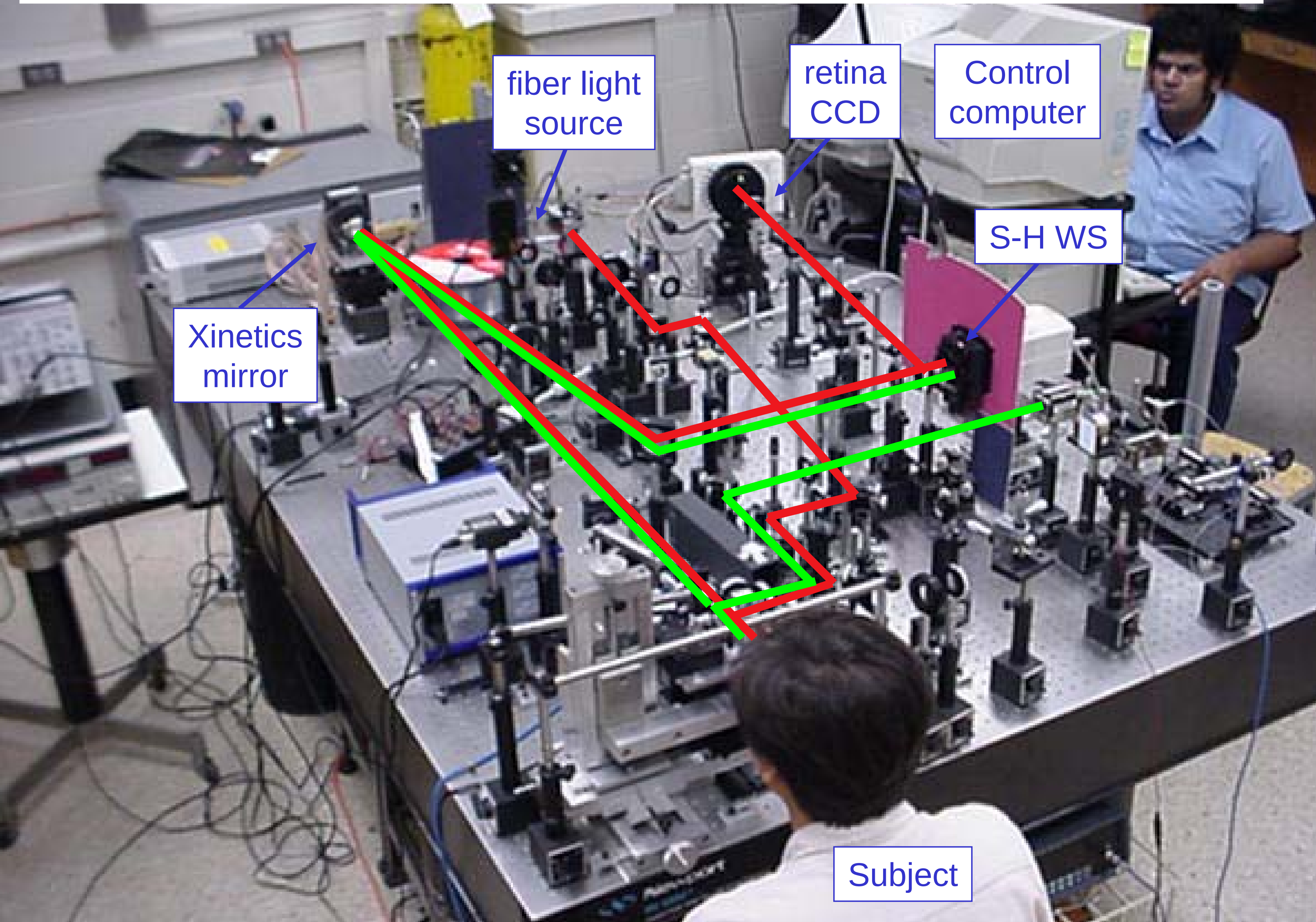

# Numerous types of wavefront sensors are available

Common path interferometer

Phasing shifting interferometer

Shack-Hartmann sensor

Shearing interferometer

Pyramid sensor

Curvature sensor

Phase diversity

etc.

# Noise sources in the Shack-Hartmann wavefront sensor

1. **Noise sources:** photon noise, CCD read noise

| | photons/lenslet |
|---|---|
| astronomy: | ~100 to close loop |
| vision: | >500,000 |

2. **Spatial sampling error:** undetected aberrations (governed by lenslet dia.)

| | lenslet dia. and spacing | |
|---|---|---|
| astronomy: | ~ $r_o$, | uniform sampling |
| vision: | ?, | ? |

3. **Temporal sampling error:** undetected aberrations (1-6 Hz) (governed by frame rate & exposure)

# Typical SH sensor parameters for the eye

1. # of lenslets: ~200 (>1/2 million photons/lenslet for <8 μW entering eye.)

2. Lenslet array: lenslet diameter = 400μm
   (17x17 for 6.8 mm pupil)
   focal length = 24mm

3. # pixels across dot core 5 to 14

4. Wavelength 633 to 850 nm

# Indiana adaptive optics retina camera

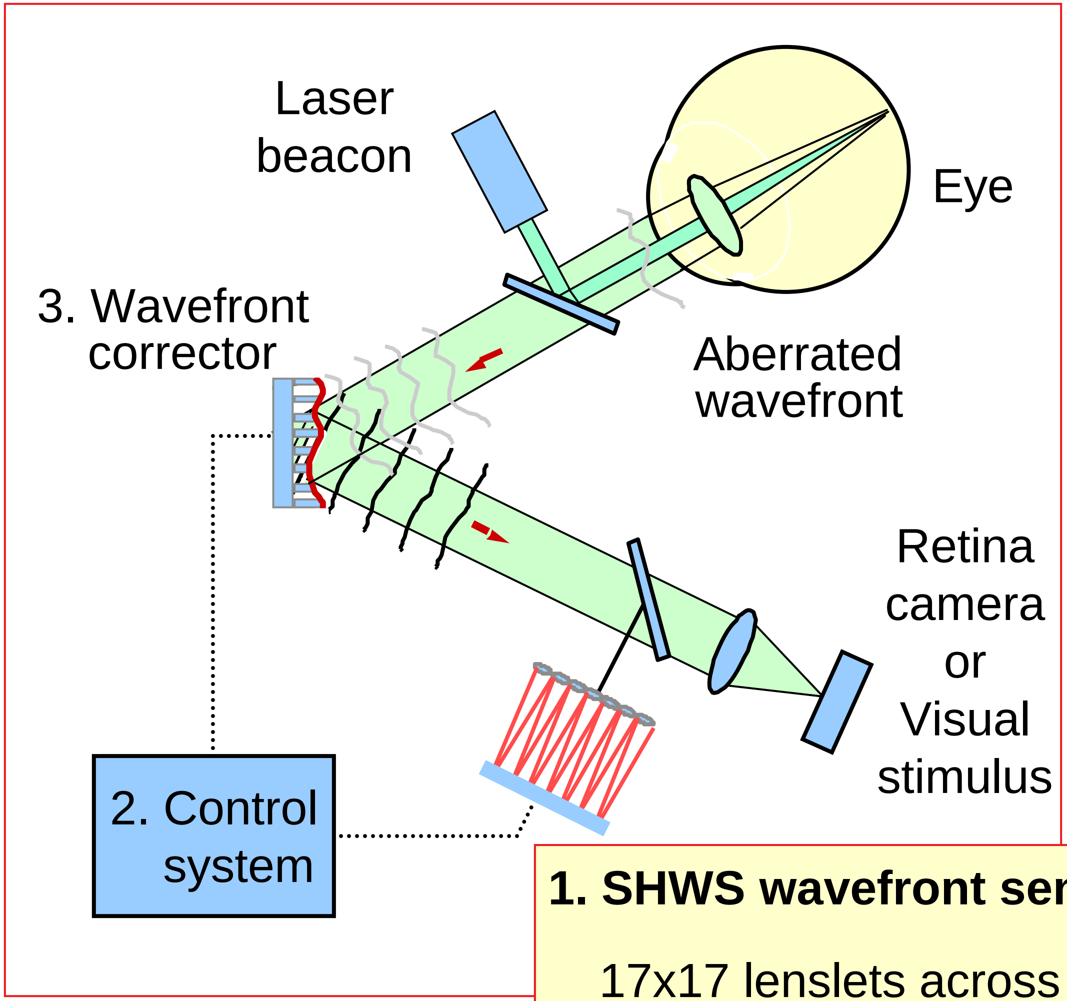


**1. SHWS wavefront sensor**

17x17 lenslets across 6.8 mm pupil
~7 pix across each focal spot
λ= 0.78 μm SLD beacon
6 μW enters eye
Inexpensive areal CCD


OKO membrane mirror

AOptix bimorph
*“fast, simple, & robust”*


Xinetics deformable mirror

Hamamatsu LC-SLM

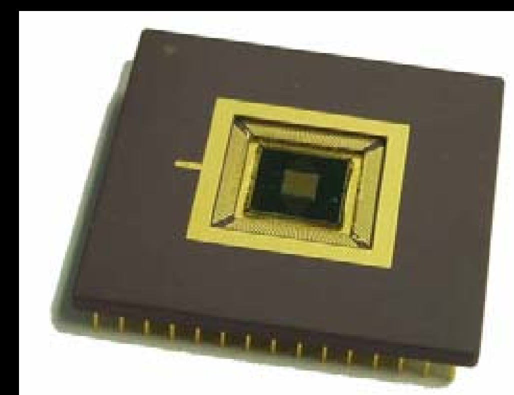

Boston Micromachines Corp.

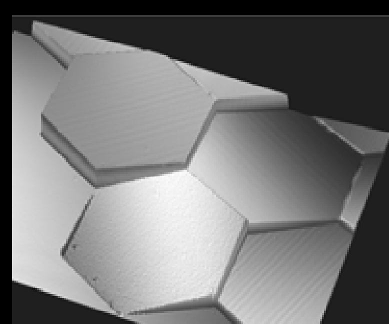

Iris AO

# Types of wavefront correctors

## (Which one is right for my application?)

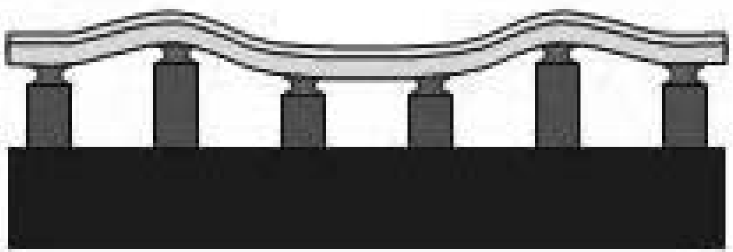

a) Discrete Actuator

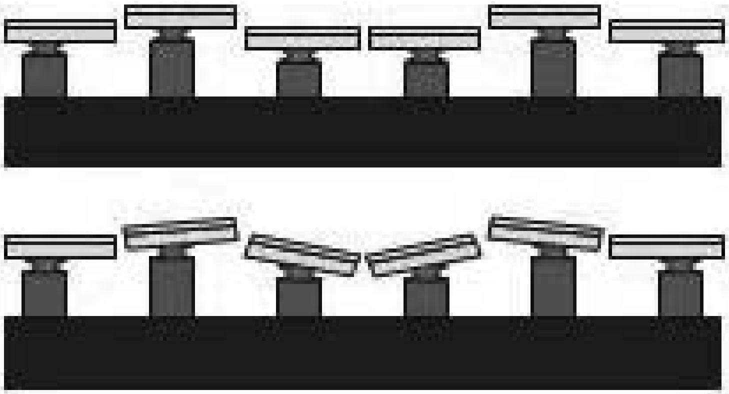

b) Segmented: Piston only and Piston/tip/tilt

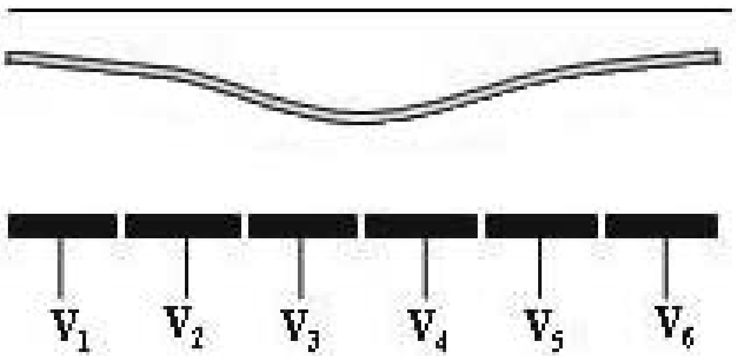


c) Membrane

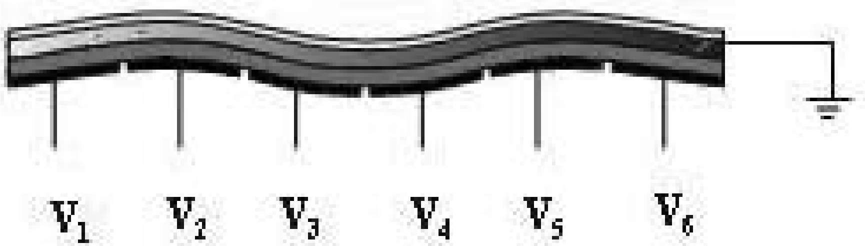


d) Bimorph

# Wavefront Corrector Performance

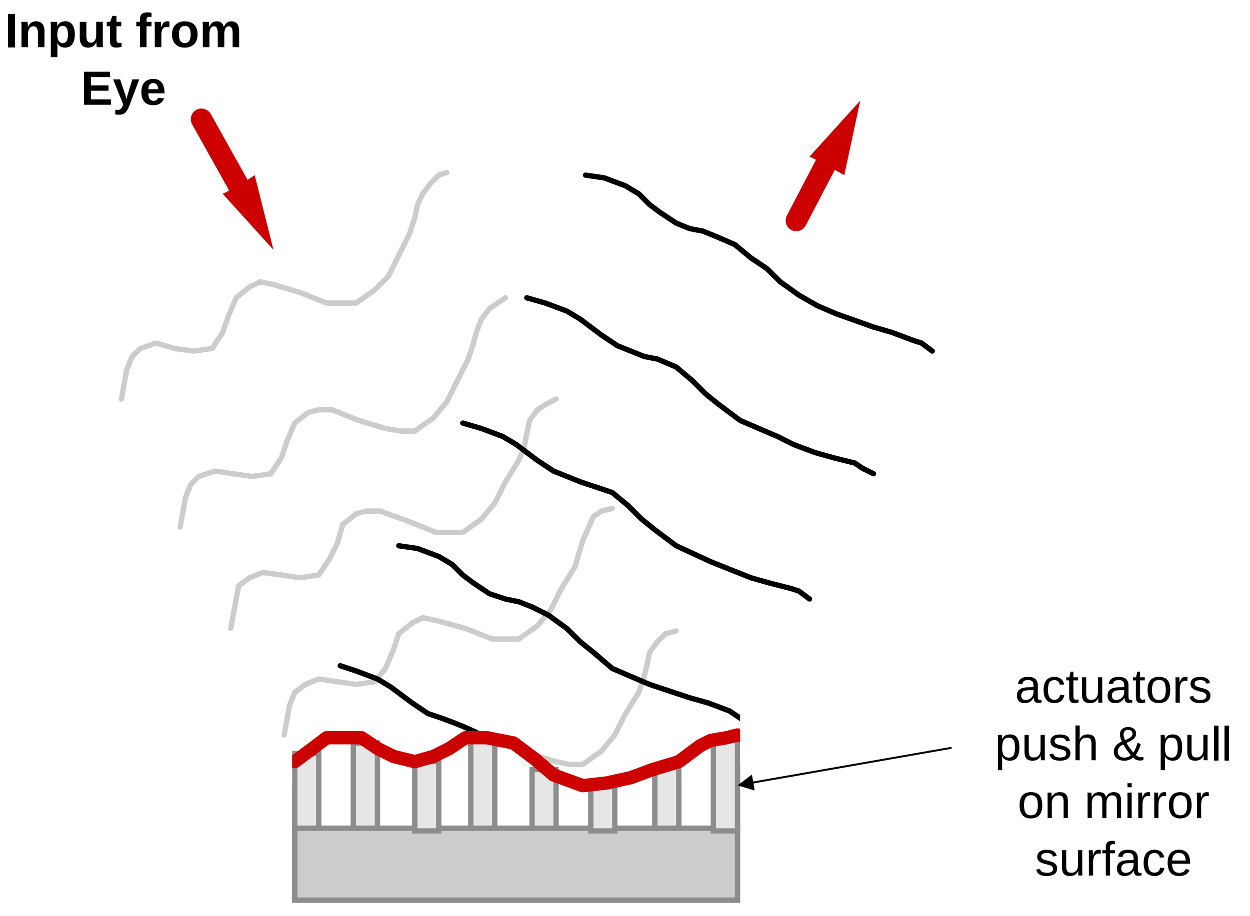


**Most important parameters:**

- Actuator stroke
- Actuator number
- Actuator influence function
- Speed
- Reflectivity
- Diameter
- Cost!

# Aberrations in two populations of 70 normal eyes for 7.5 mm pupil

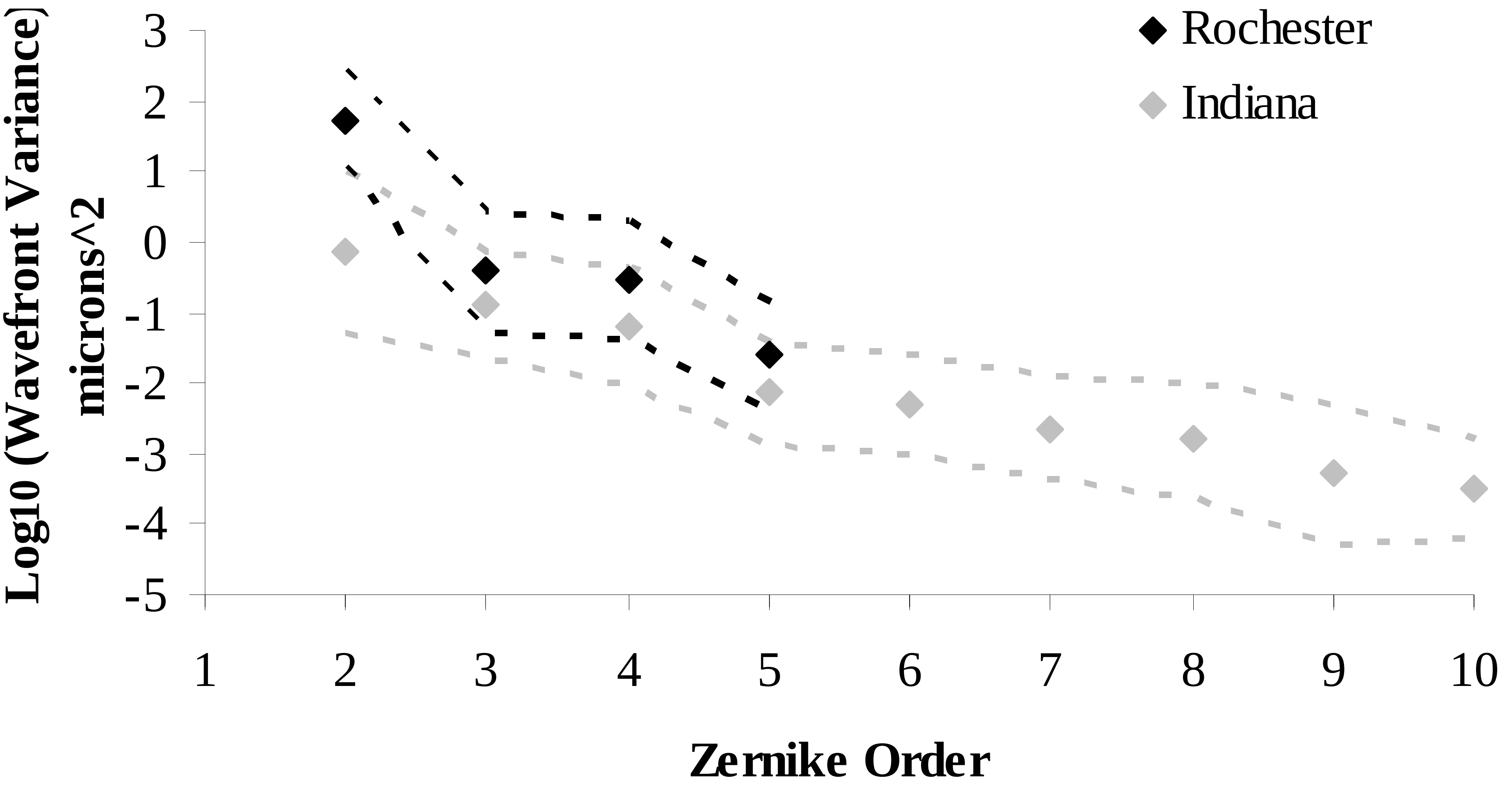

# P-V wavefront error for 7.5 mm pupil

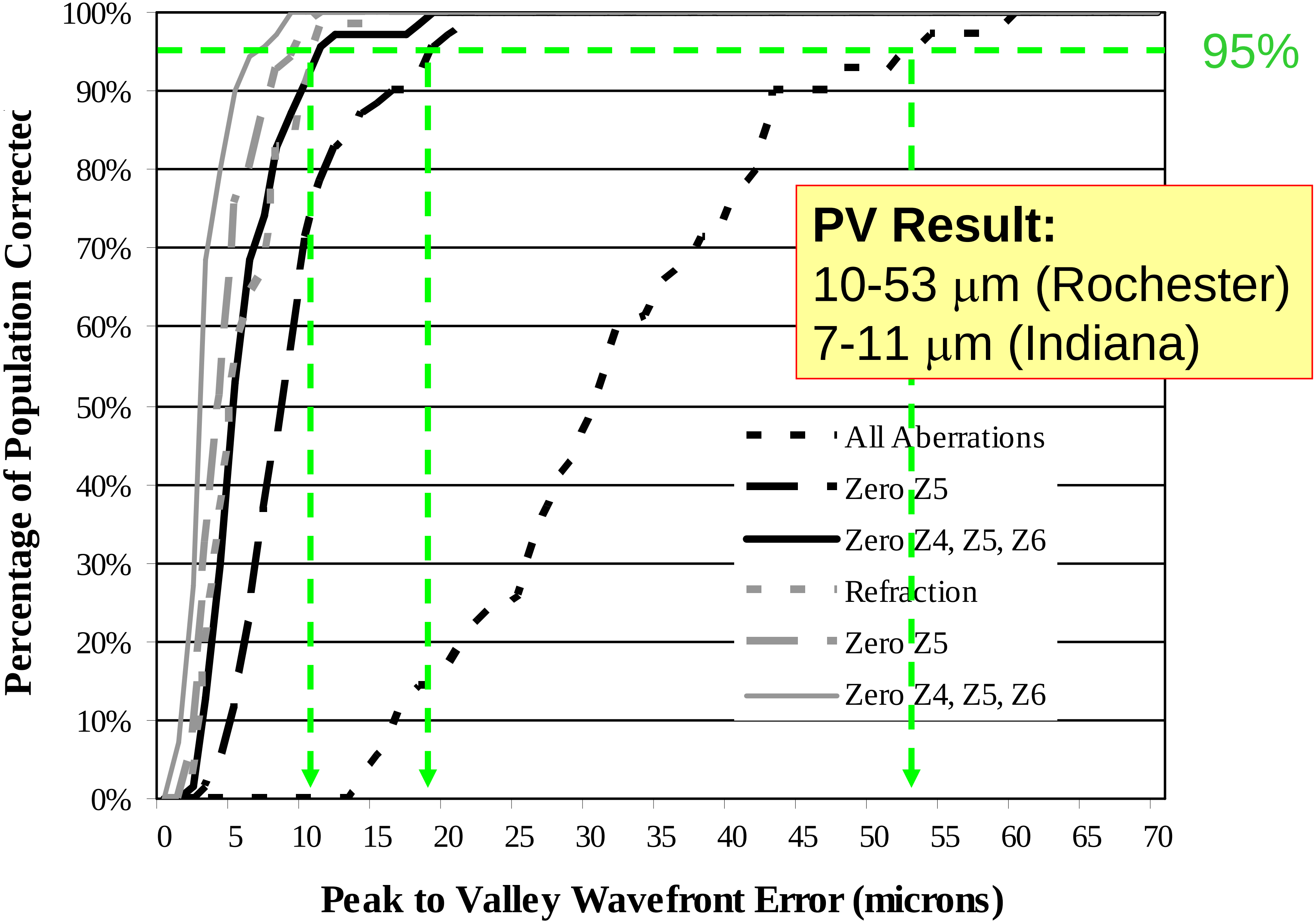

# Discrete actuator deformable mirrors

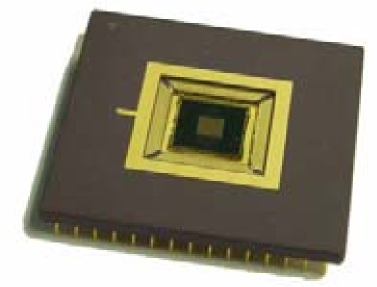


**Diff lim result: >14 (Roch), 11-14 (Ind)**

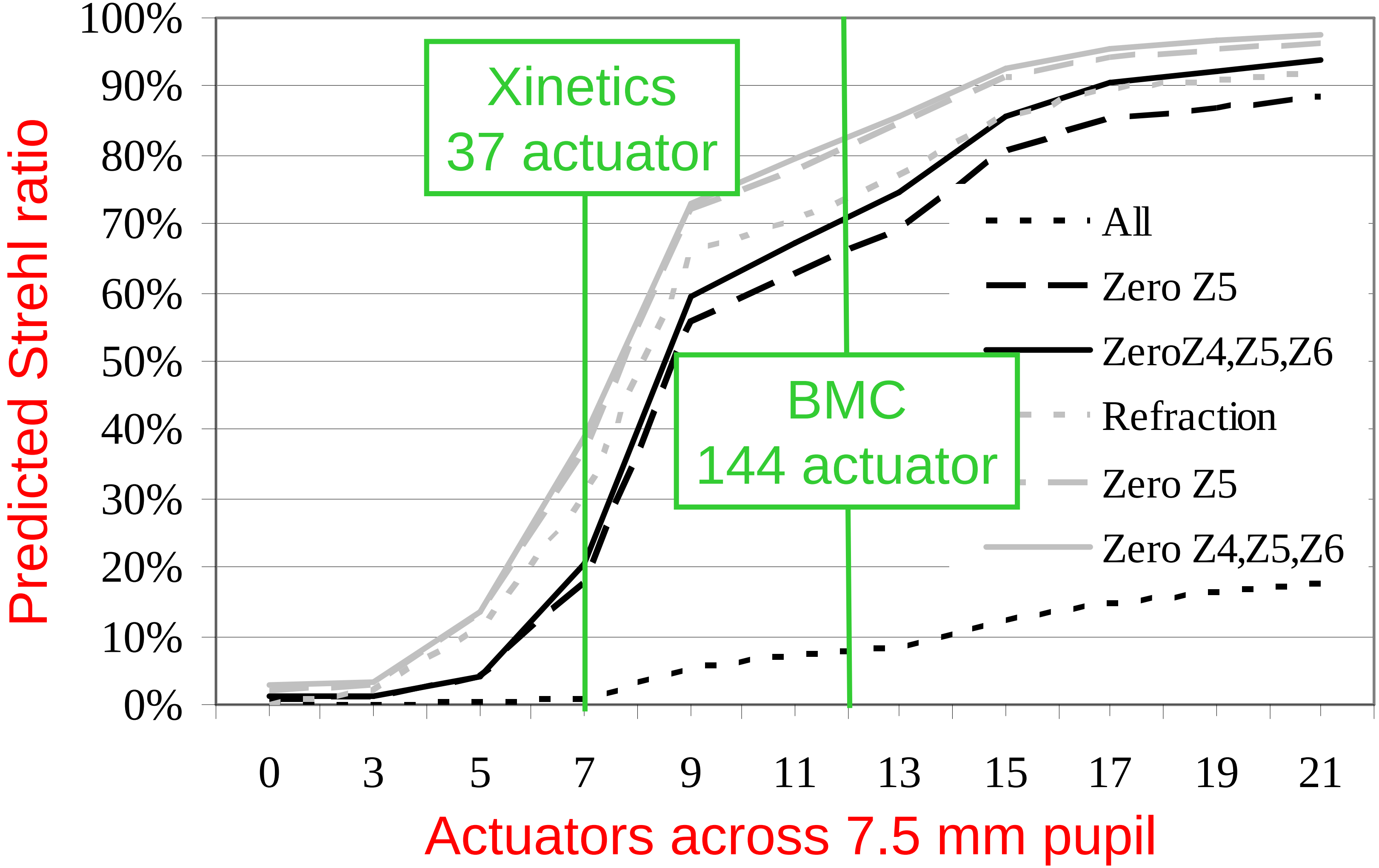

# Piston segmented correctors

**Diff lim result: >90 (Roch), 45-85 (Ind)**

480x480 segments

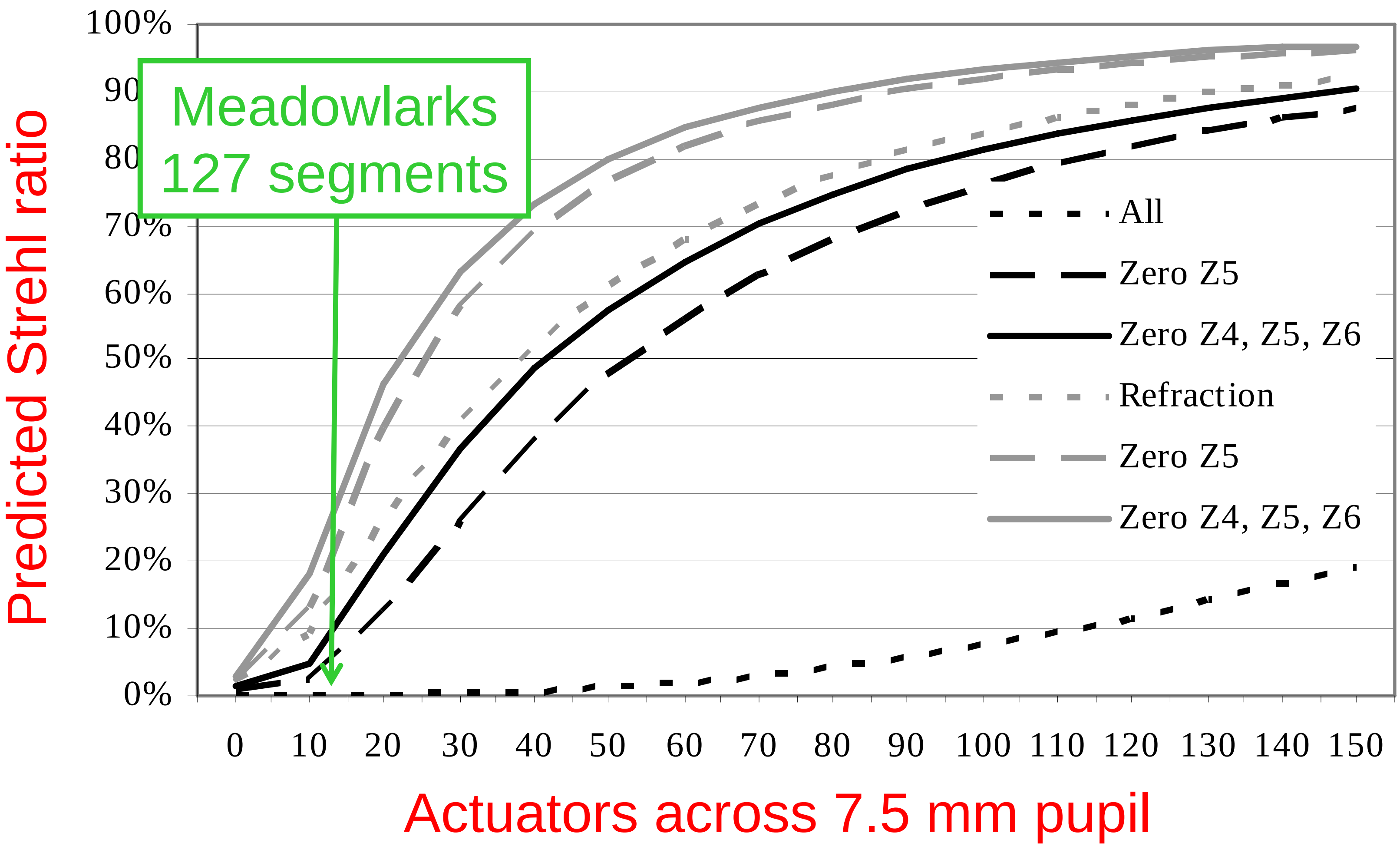

# Piston/tip/tilt segmented correctors

Diff lim result: 12-19 (Roch), 9-10 (Ind)

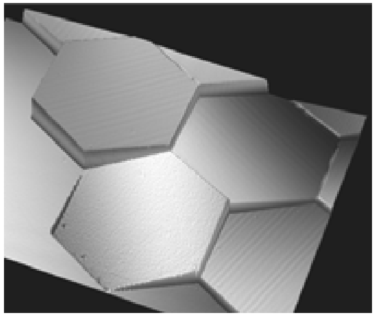

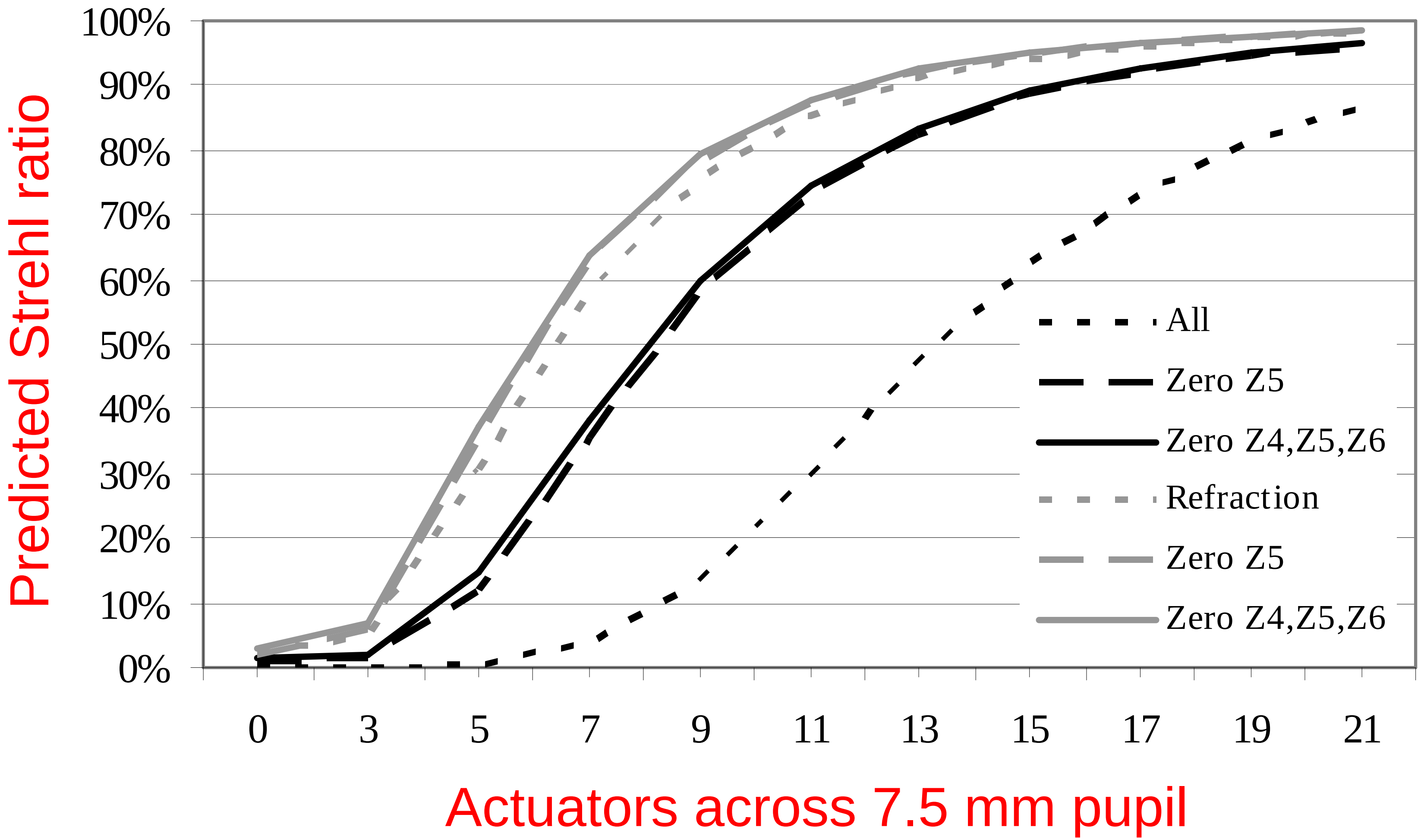

# Predicted performance for OKO and AOptix mirrors

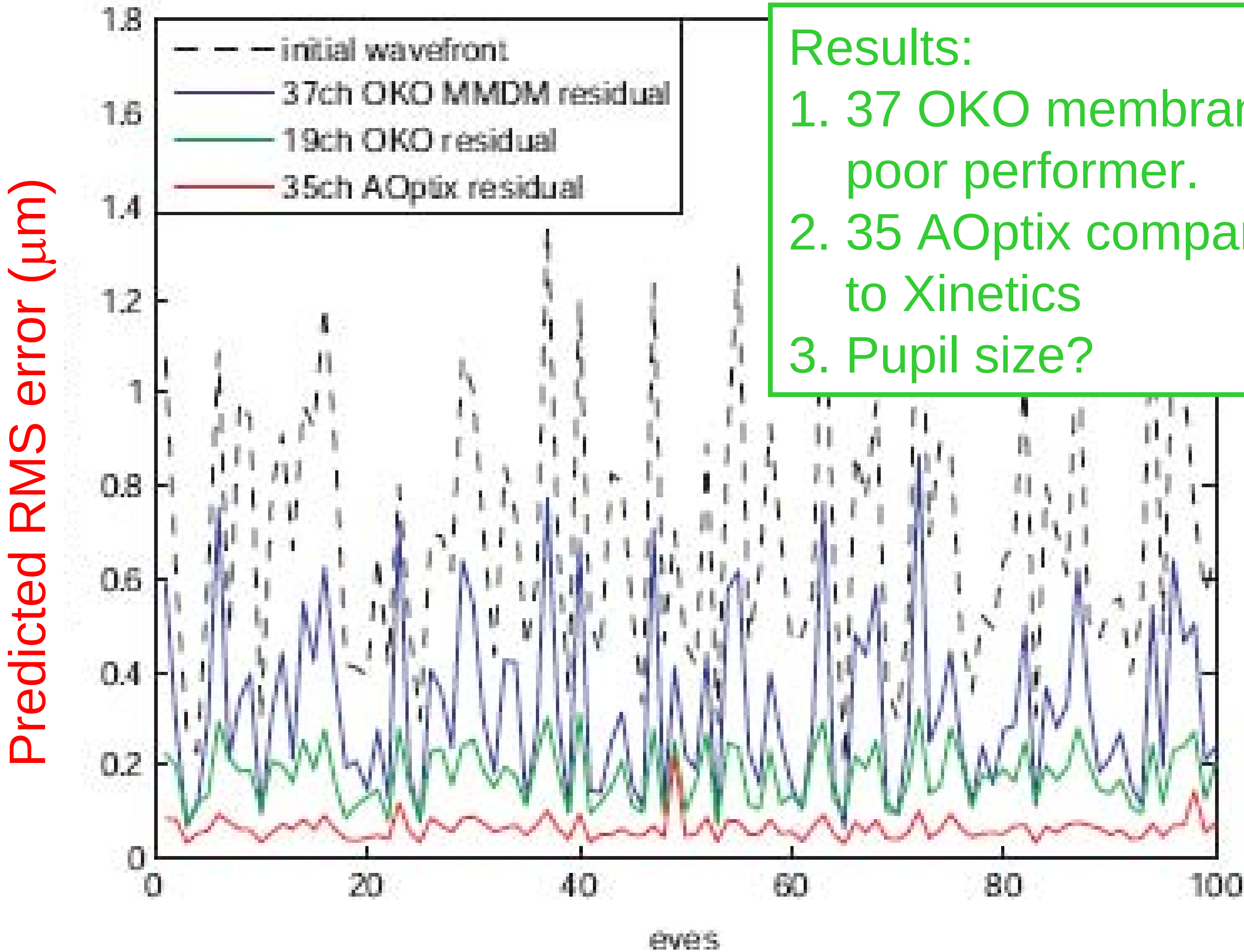


Results:

1. 37 OKO membrane poor performer.
2. 35 AOptix comparable to Xinetics
3. Pupil size?

Dalimier E, Dainty C. Comparative analysis of deformable mirrors for ocular adaptive optics. *Opt Express.* 2005;13:4275-4285

# Desired parameters for the wavefront corrector

| | |
|---|---|
| Temporal Bandwidth | 1-6 Hz fluctuations in the eye |
| Reflectivity | >90% (400-900 nm) |
| Physical size | 4 - 8 mm |
| Mirror Stroke<br>(7.5-mm pupil, 95% population) | 10-53 μm (Rochester)<br>7-11 μm (Indiana) |
| # of actuators or segments across 7.5 mm pupil (for 80% Strehl) | > 14 (Roch), 11-14 (Ind) Discrete actuator<br>>> 90 (Roch), 45-85 (Ind) Piston-only segmented<br>12-19 (Roch), 9-10 (Ind) Piston/tip/tilt segmented<br><br>>> 37 OKO membrane<br>>19 OKO piezoelectric<br>~35 AOptix |

# Indiana adaptive optics retina camera

**3. Xinetics wavefront corrector**

37 actuators fill 6.8 mm pupil
4 μm stroke
Predicted Strehl = 0.2-0.4 (7.5 mm)

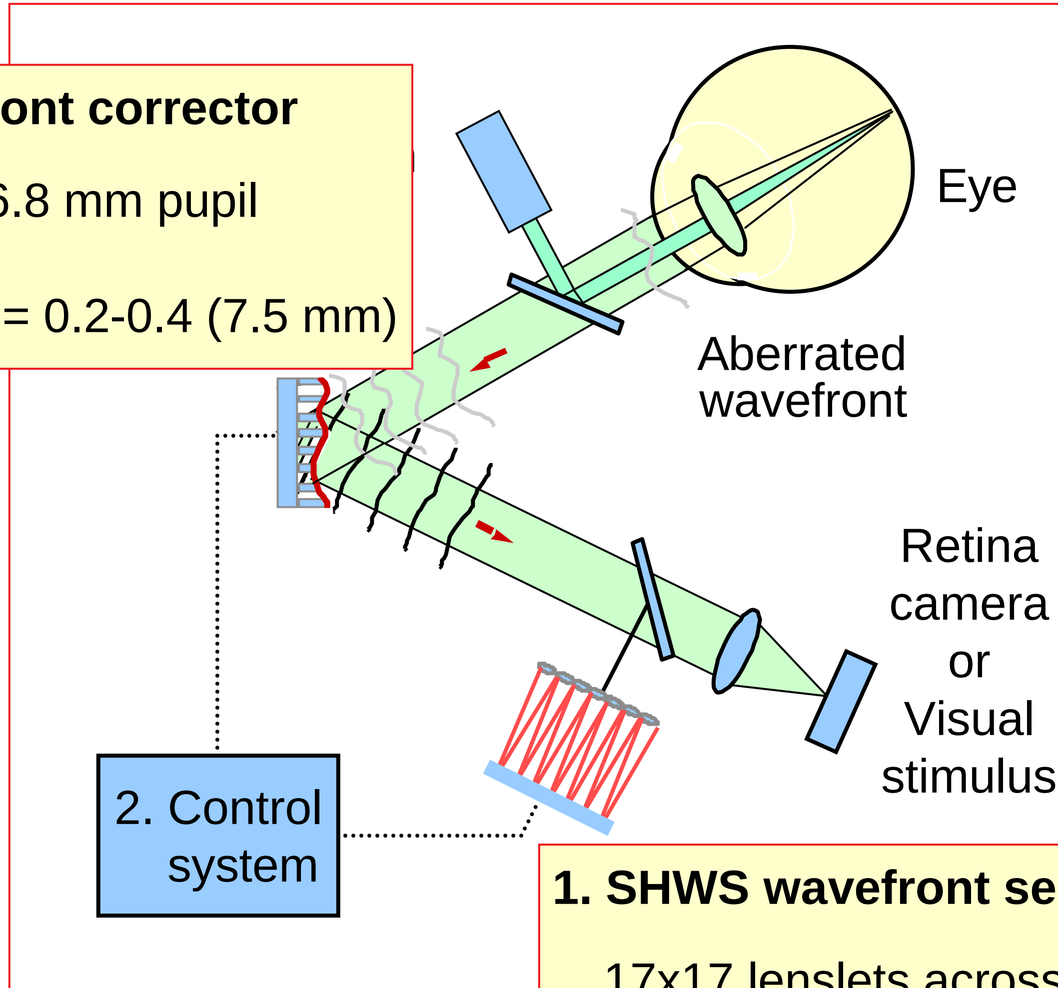


**1. SHWS wavefront sensor**

17x17 lenslets across 6.8 mm pupil
~7 pix across each focal spot
$\lambda$= 0.78 μm SLD beacon
6 μW enters eye
Inexpensive areal CCD

# Direct slope reconstruction method

$$[\,S\,] = [\,F\,]\;[\,M\,]$$

- $[S]$: Measured sensor slopes (m,1)
- $[F]$: Response matrix for the mirror-sensor system (m,n)
- $[M]$: Mirror Voltages (n,1)

$$[\,M\,] = \underbrace{([F]^T[F])^{-1}\,[F]^T}_{\text{Least squares solution to inverse}}\,[\,S\,]$$

Least squares solution to inverse

# Temporal power spectra of the wavefront disturbance without and with dynamic correction

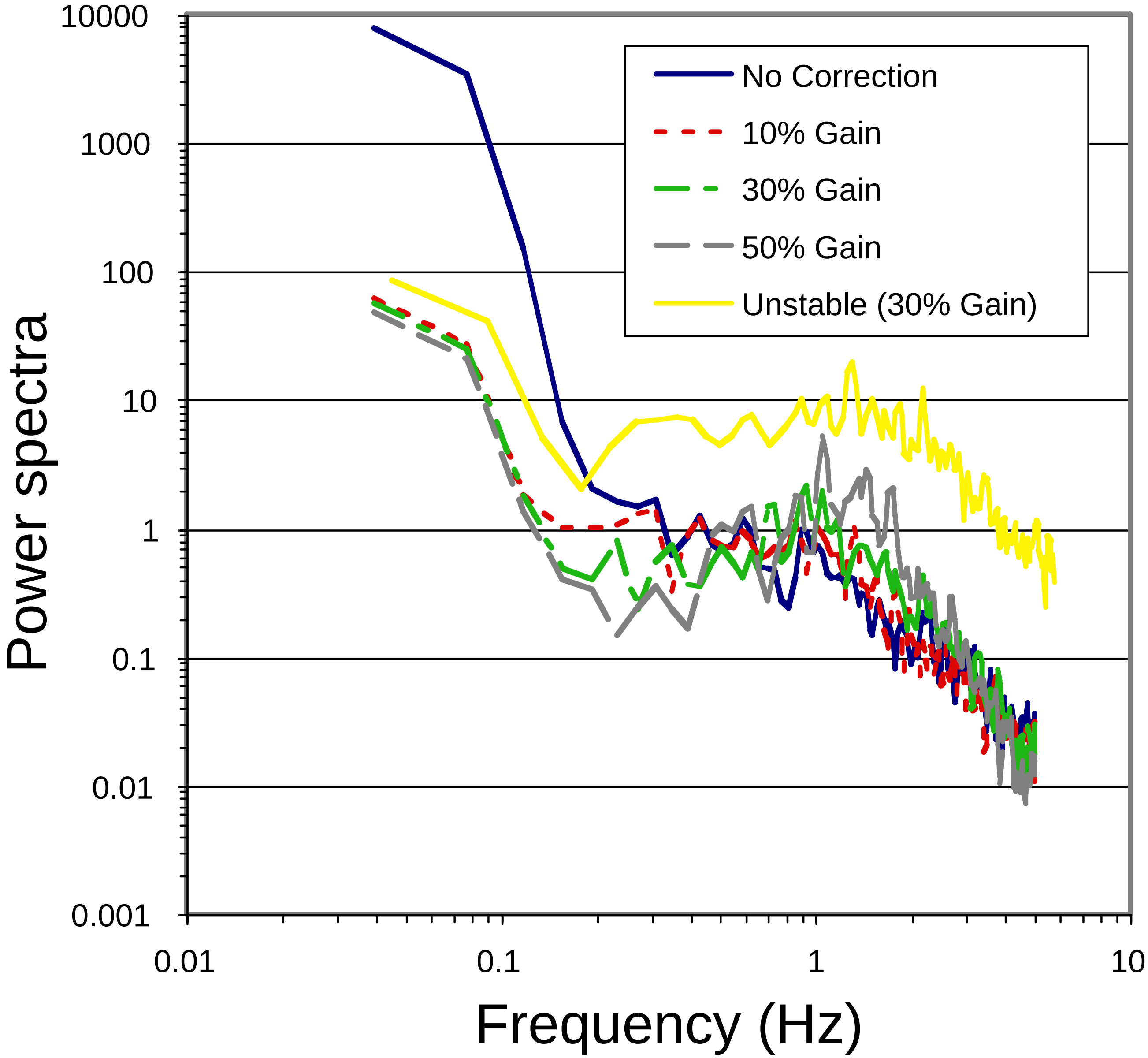

**Power rejection magnitude** = $\frac{\text{power spectra with AO}}{\text{power spectra w/o AO}}$

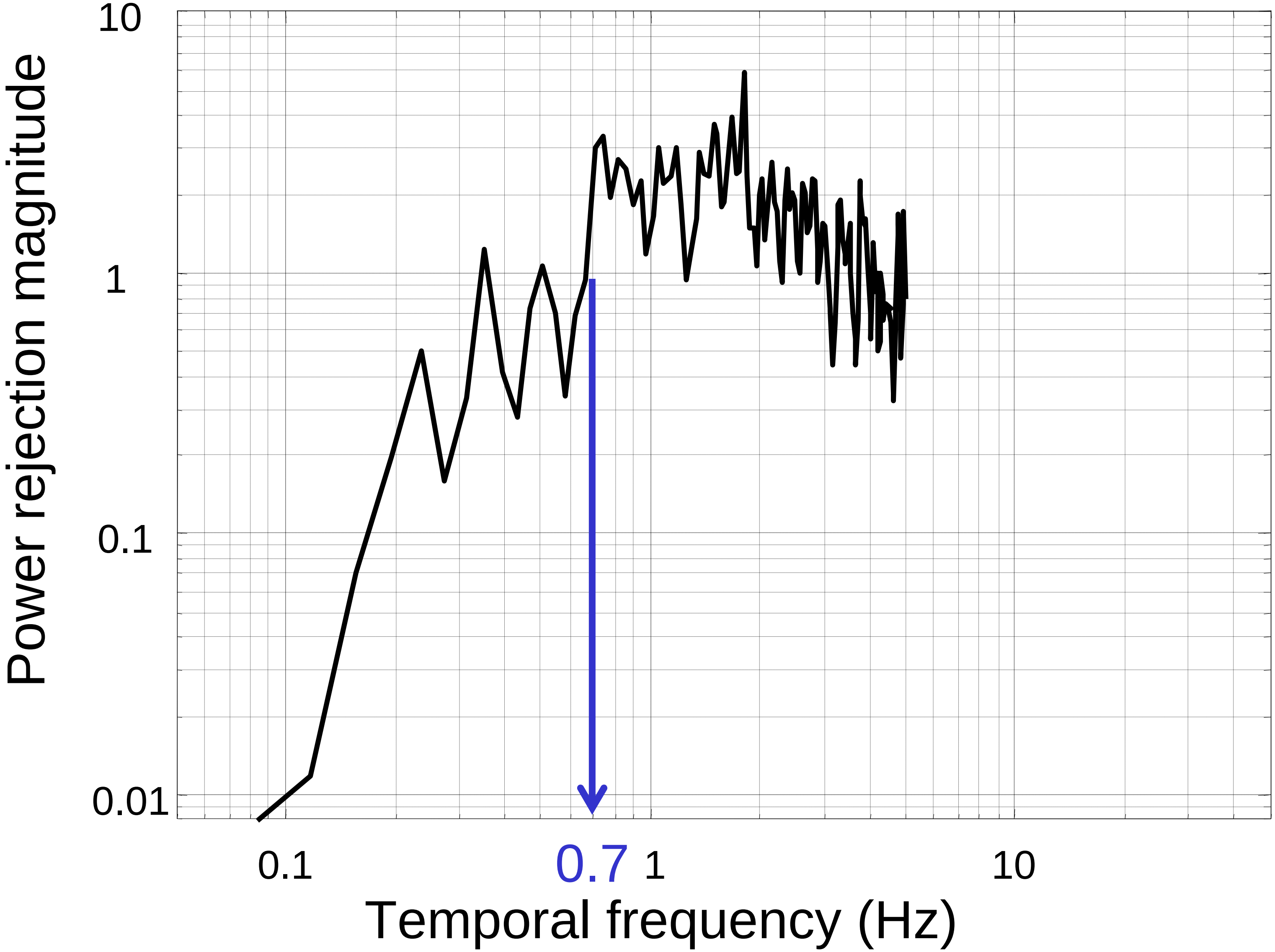

# Schematic of a closed-loop AO system

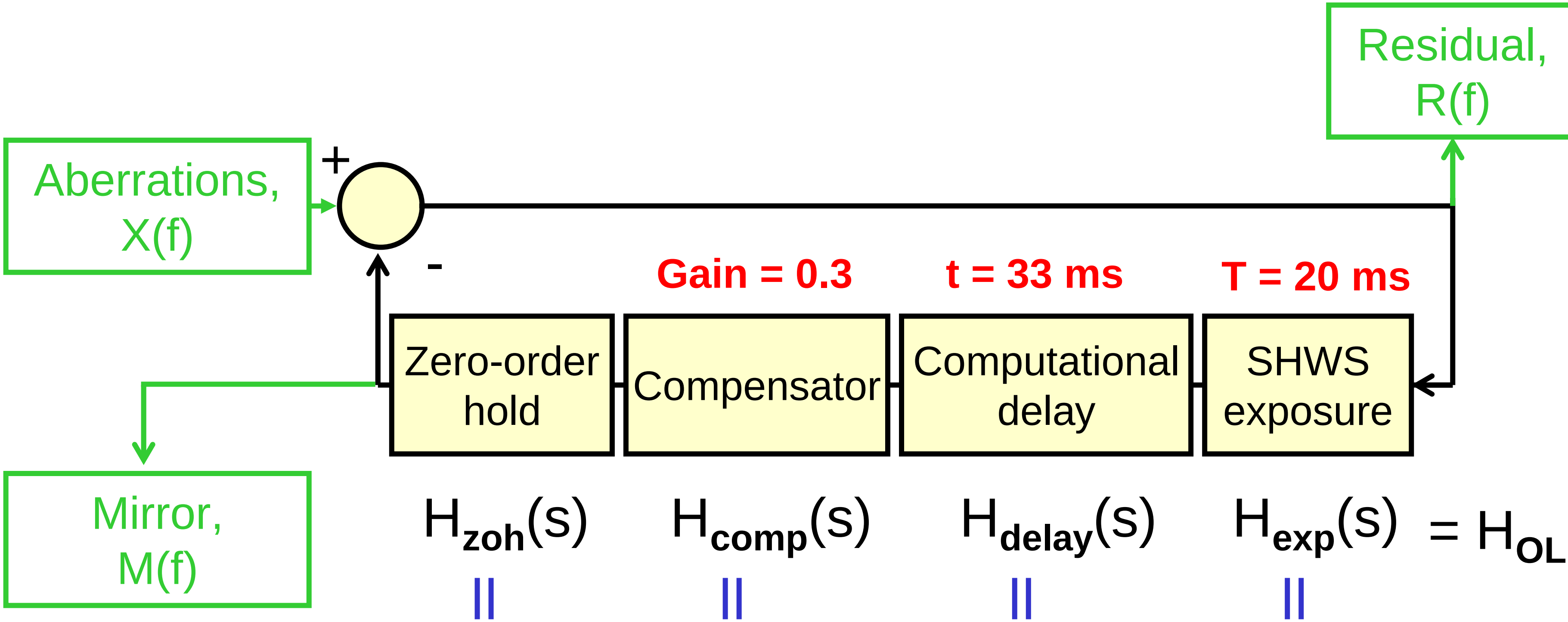


$$H_{zoh}(s) \, H_{comp}(s) \, H_{delay}(s) \, H_{exp}(s) = H_{OL}(s)$$

$$H_{zoh}(s) = \frac{1-e^{-sT}}{s}, \quad H_{comp}(s) = \frac{G}{1-e^{-sT}}, \quad H_{delay}(s) = e^{-st}, \quad H_{exp}(s) = \frac{1-e^{-sT}}{sT}, \quad s=i2\pi f$$

$$\sqrt{\text{Power rejection curve}} = \text{Closed-loop transfer function} = H_{CL}(s) = \frac{R(s)}{X(s)} = \frac{1}{1 + H_{OL}(s)}$$

# Predicted and measured power rejection magnitude of the Indiana AO retina camera

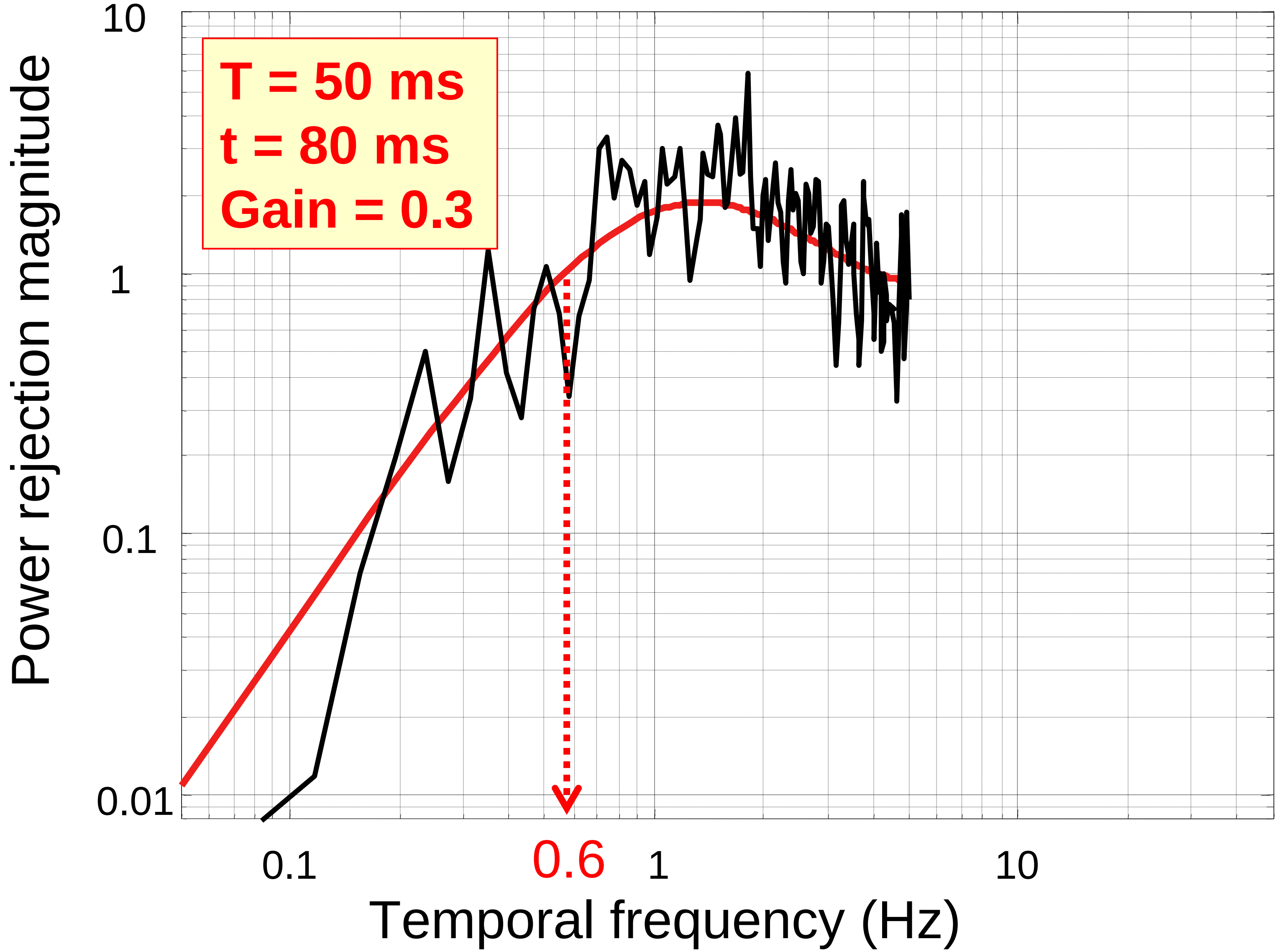

# How does the AO perform during & immediately after an eye blink?

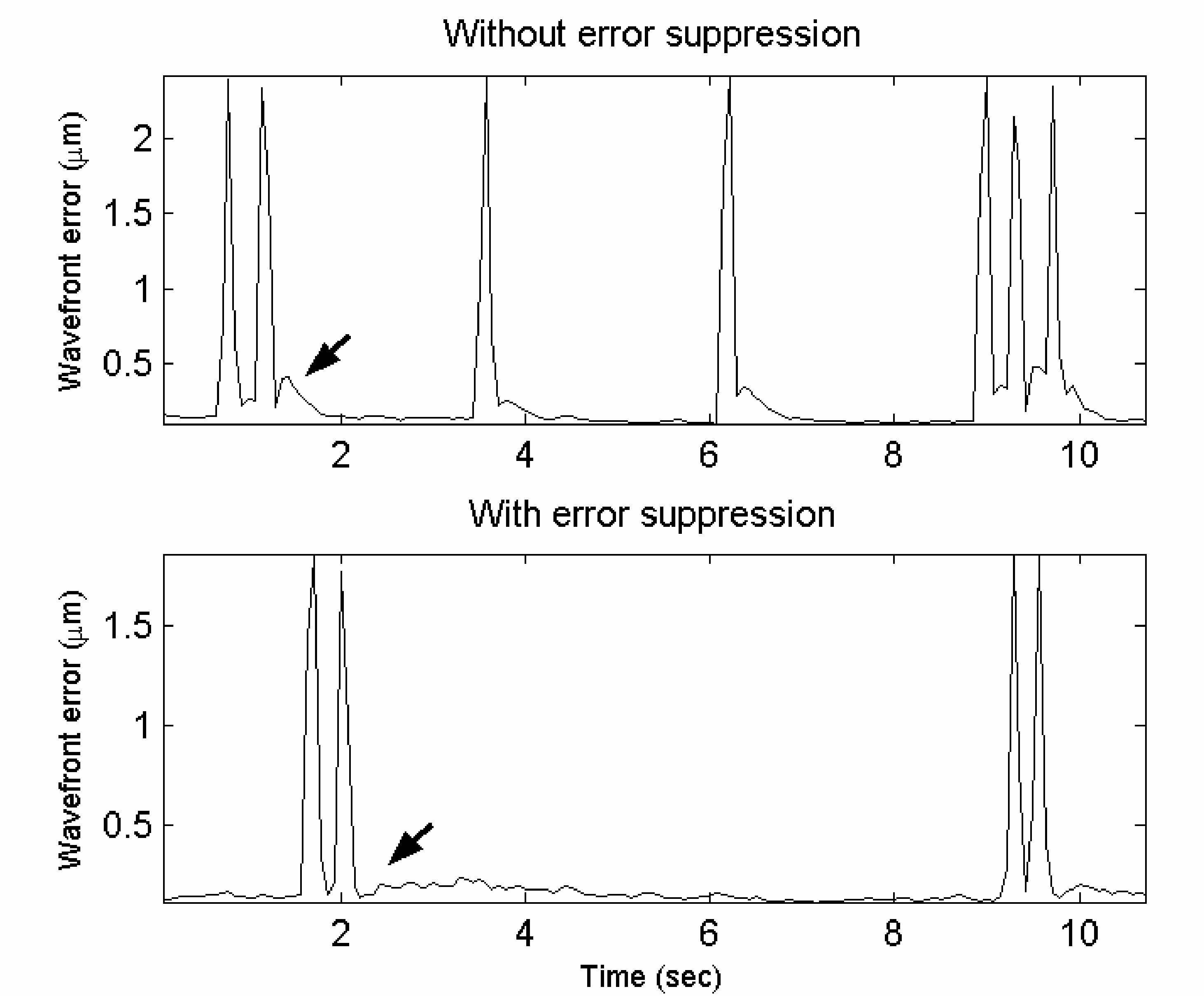

# Impact of freezing the middle five actuators during a dynamic correction was found negligible

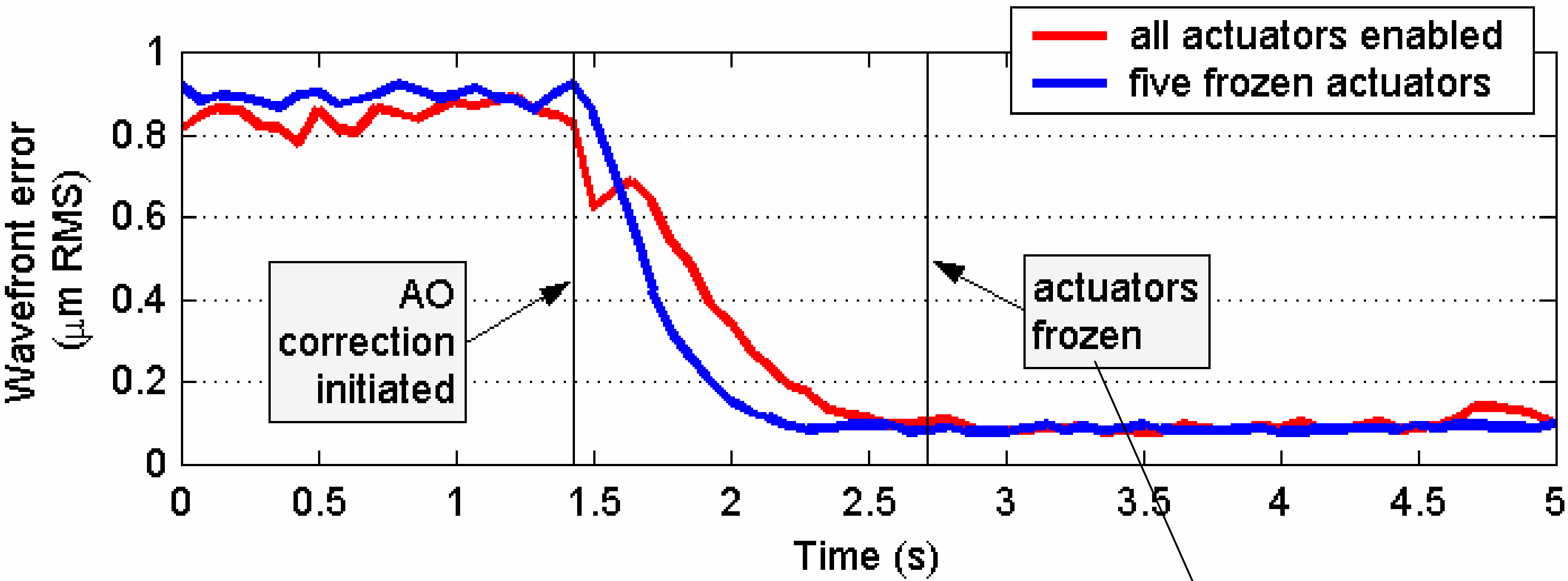


**(6.8 mm pupil, $\lambda$= 0.78 μm)**

# Time stamping SHWS measurements permits more accurate deconvolution.

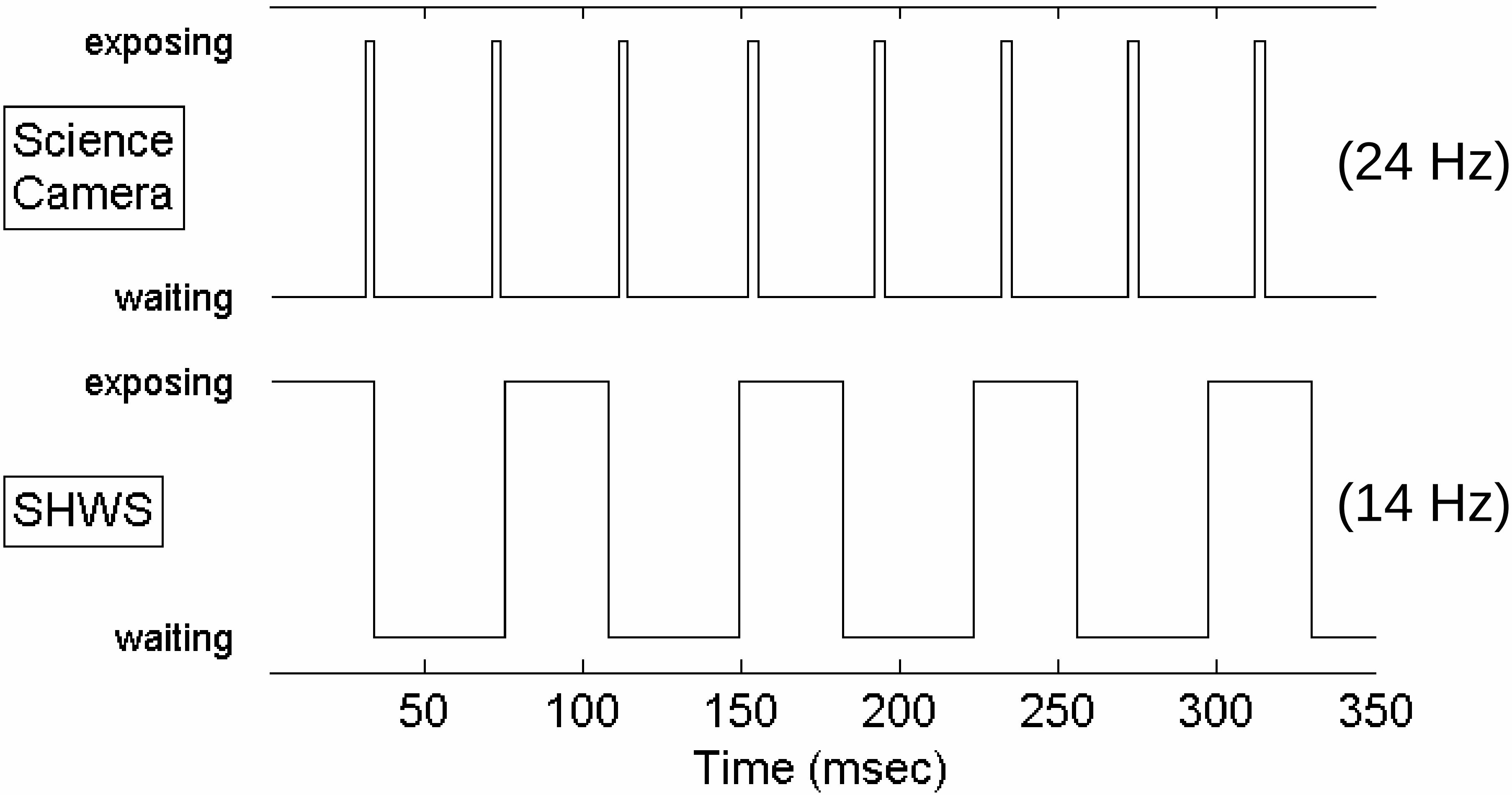


Timing diagram of concurrent SHWS measurements (14 Hz) and acquisition of science images (24 Hz) as obtained on one subject's eye

# Indiana adaptive optics retina camera

**3. Xinetics wavefront corrector**

37 actuators fill 6.8 mm pupil
4 μm stroke
Predicted Strehl = 0.2-0.4 (7.5 mm)

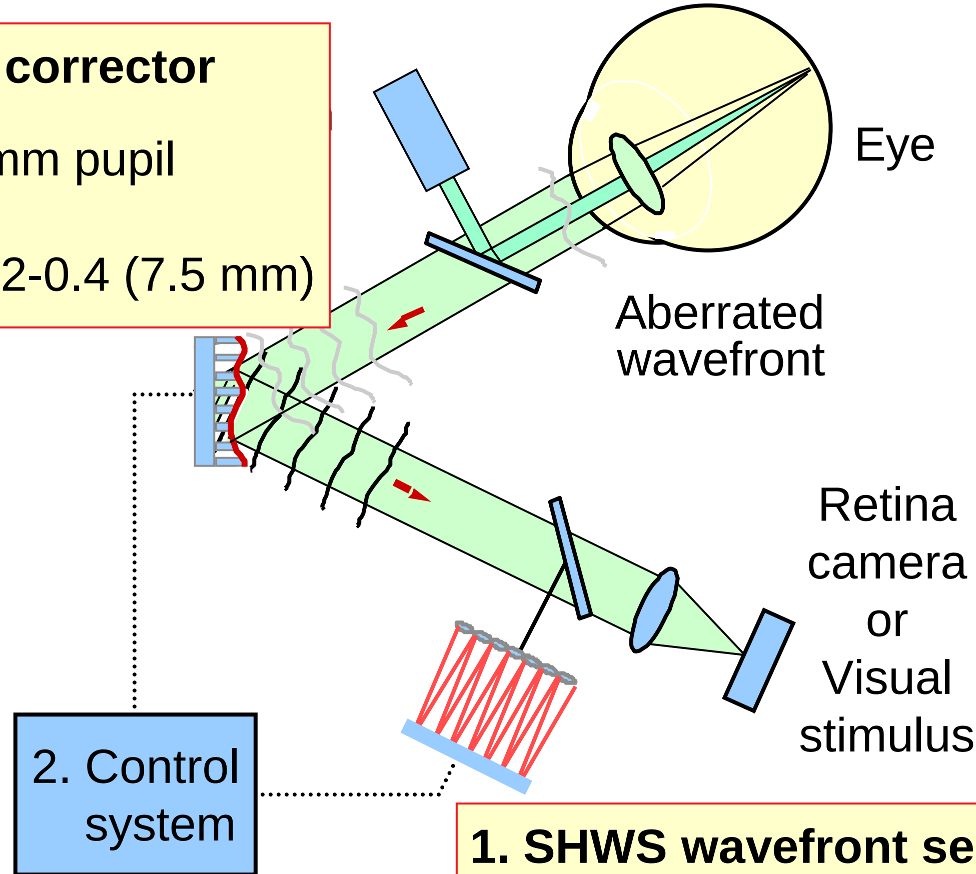


**2. Control system**

Zonal reconstructor (direct slope)
0.6 Hz cutoff frequency

**1. SHWS wavefront sensor**

17x17 lenslets across 6.8 mm pupil
~7 pix across each focal spot
λ= 0.78 μm SLD beacon
6 μW enters eye
Inexpensive areal CCD

# Dynamic correction in one subject's eye as revealed by measured PSF

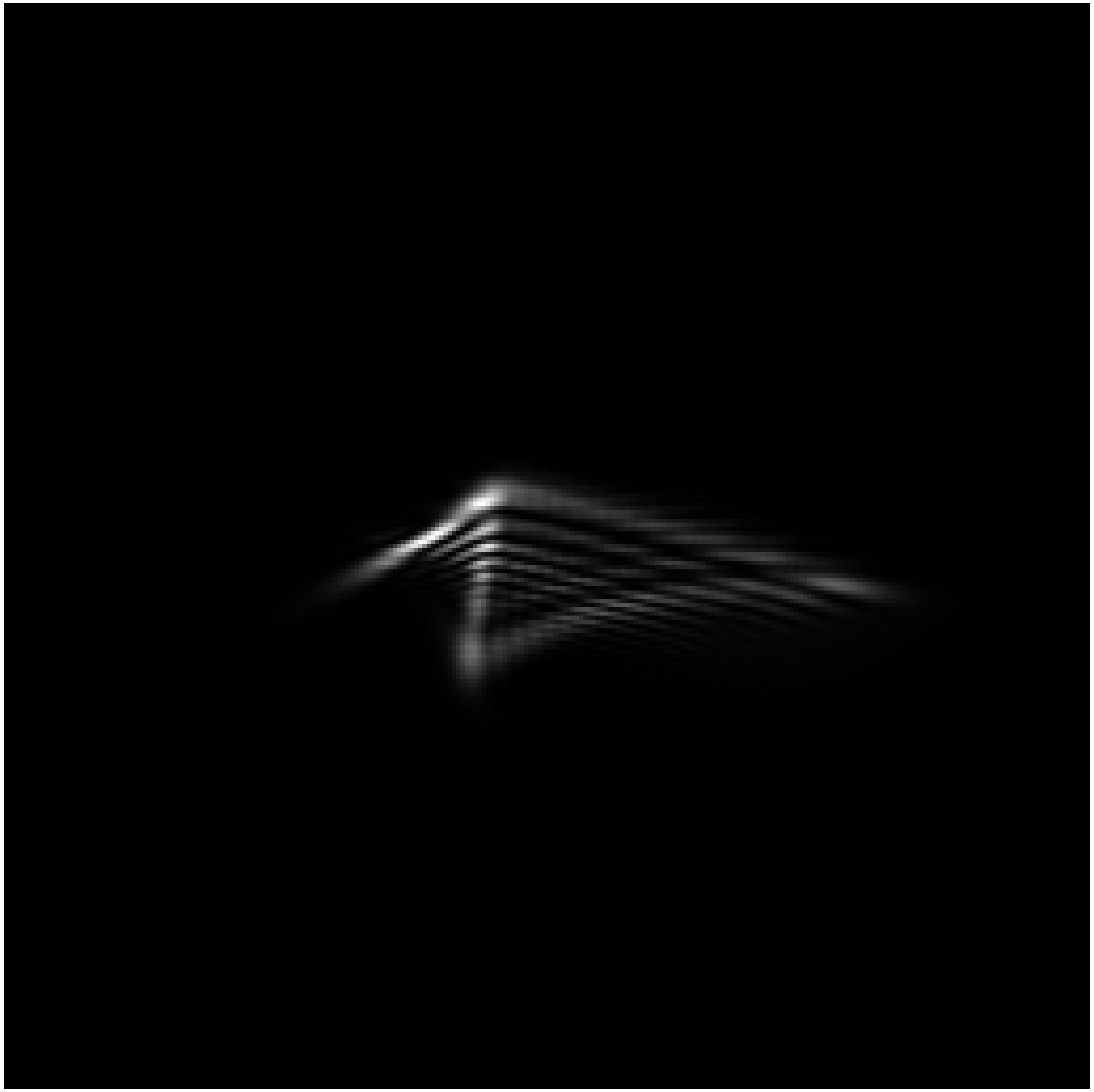

80 frame video

- λ= 0.78 μm
- 6.8 mm pupil
- 10% Gain
- 21 Hz

**Before correction:**

1.6 μm RMS

**After correction:**

0.16 μm RMS

- 27 frames to converge

# Dynamic correction in one subject's eye as revealed by measured PSF

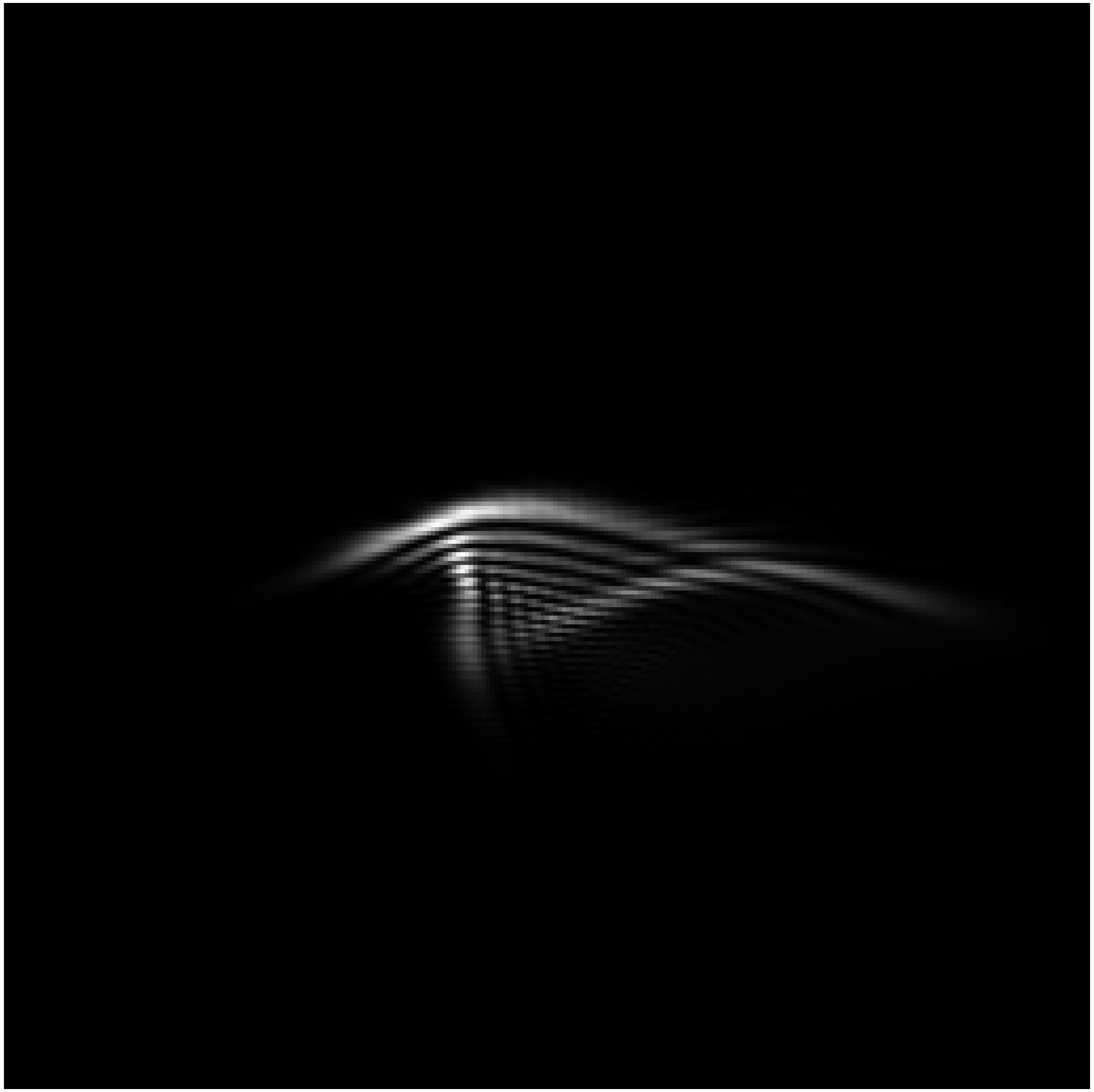

80 frame video

- λ= 0.78 μm
- 6.8 mm pupil
- 30% Gain
- 21 Hz

**Before correction:**

1.6 μm RMS

**After correction:**

0.16 μm RMS

- 6 frames to converge

# Dynamic correction in one subject’s eye as revealed by measured total RMS

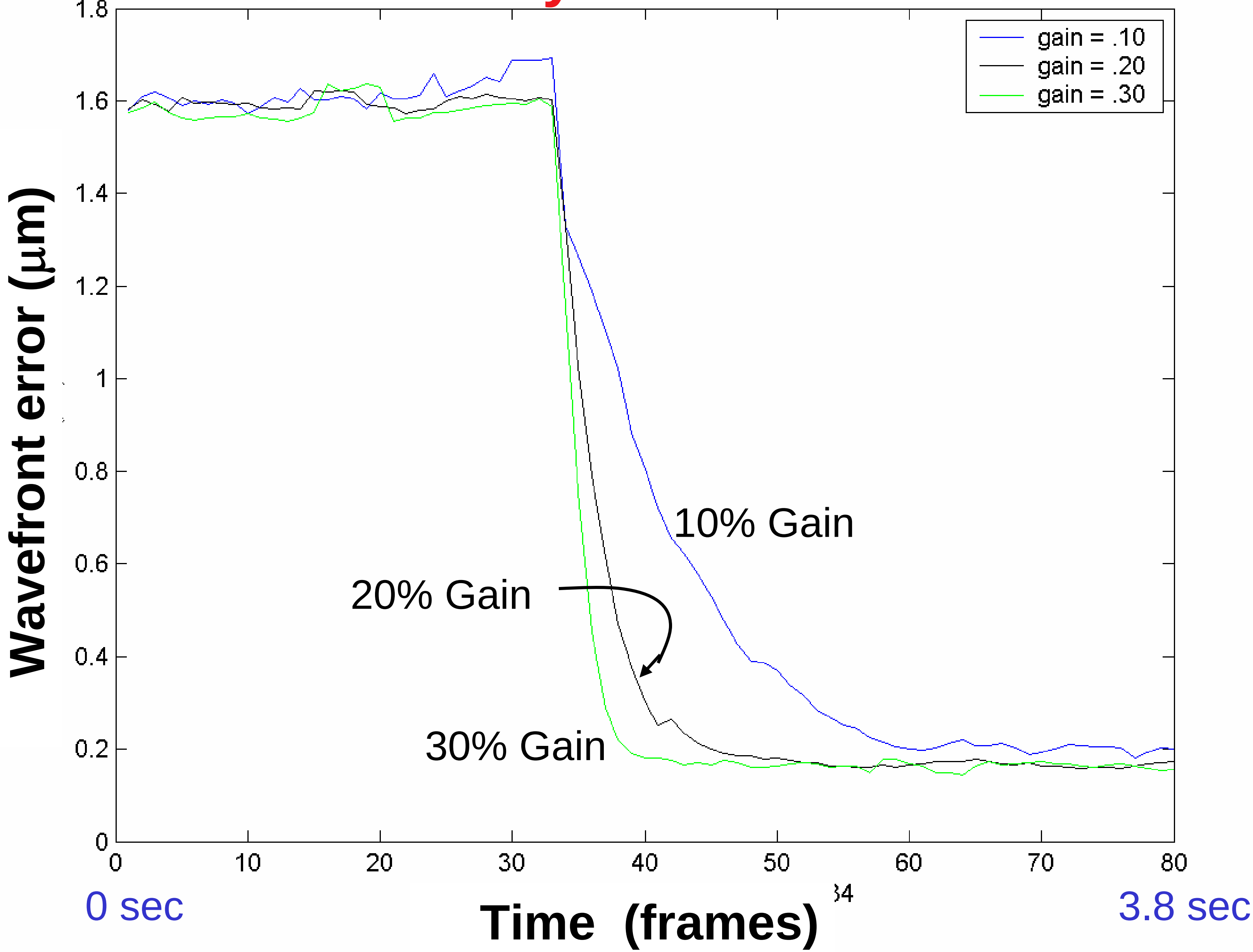

# How accurate is the measured PSF?

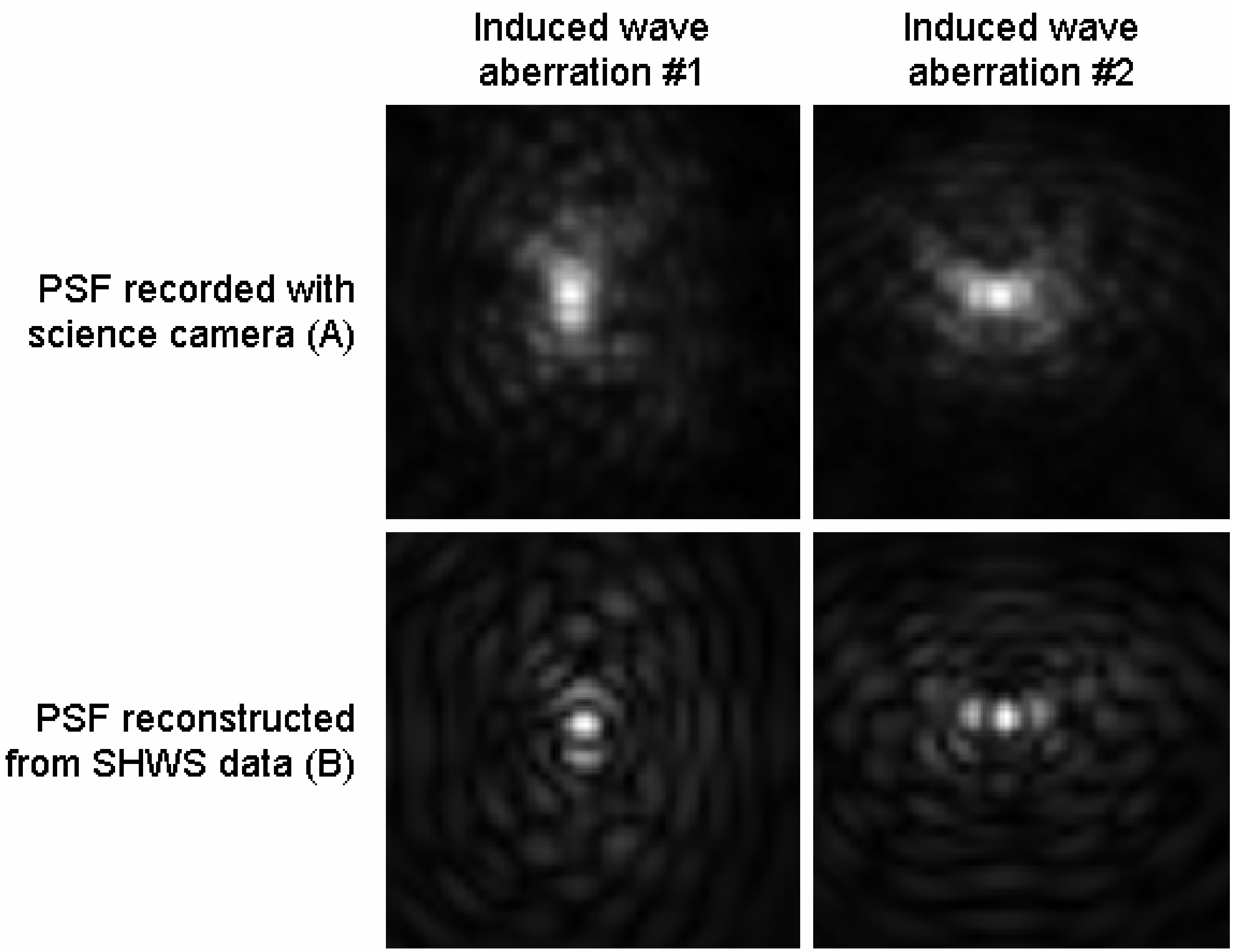

# Turning on the AO during a 10 Hz video of the cone mosaic

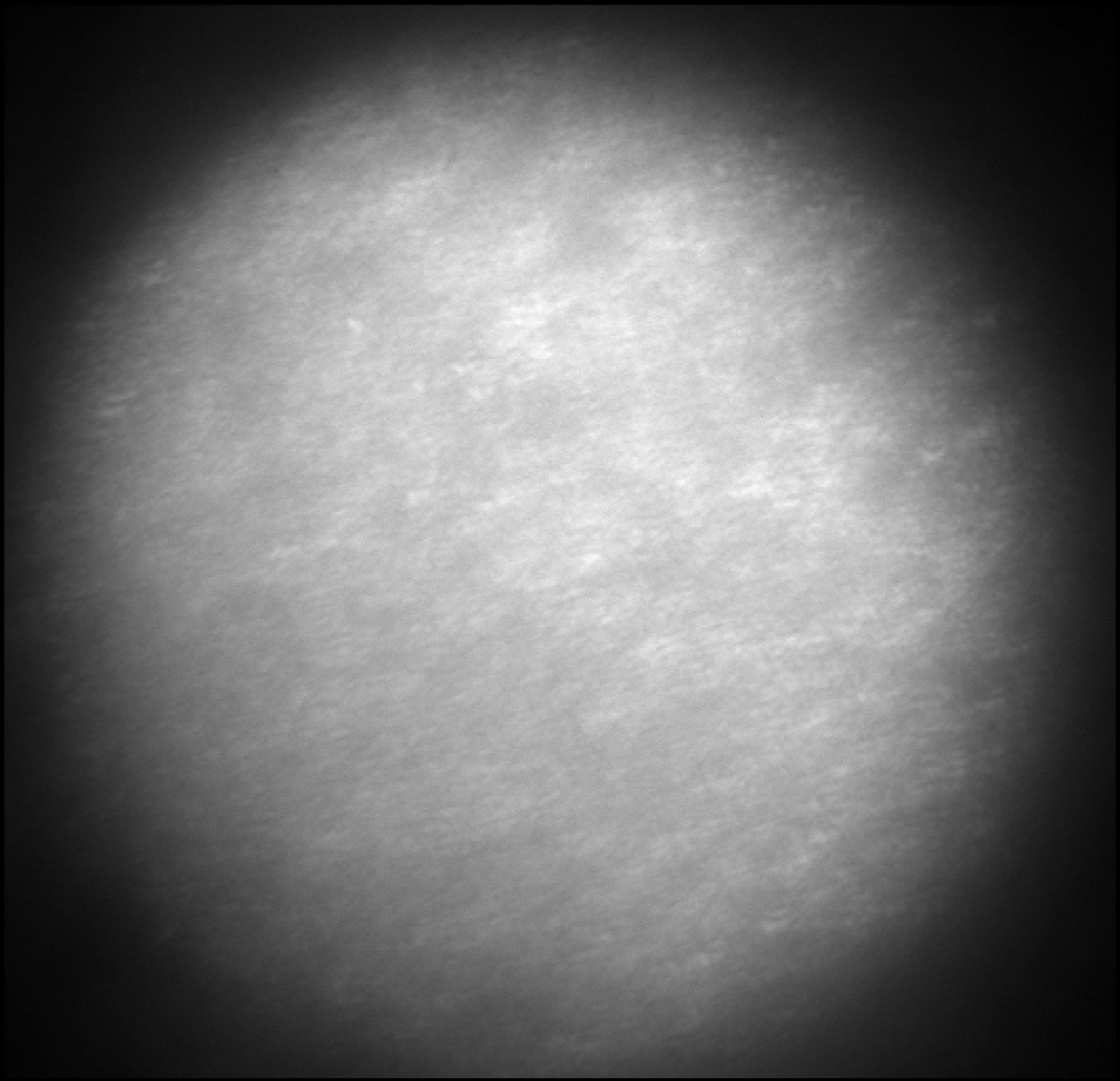

- Video rate: 10 fps
- 2° FOV
- 1° ecc.
- AO correcting at 15 Hz
- 6.0 mm pupil

# Cone images in one subject's eye

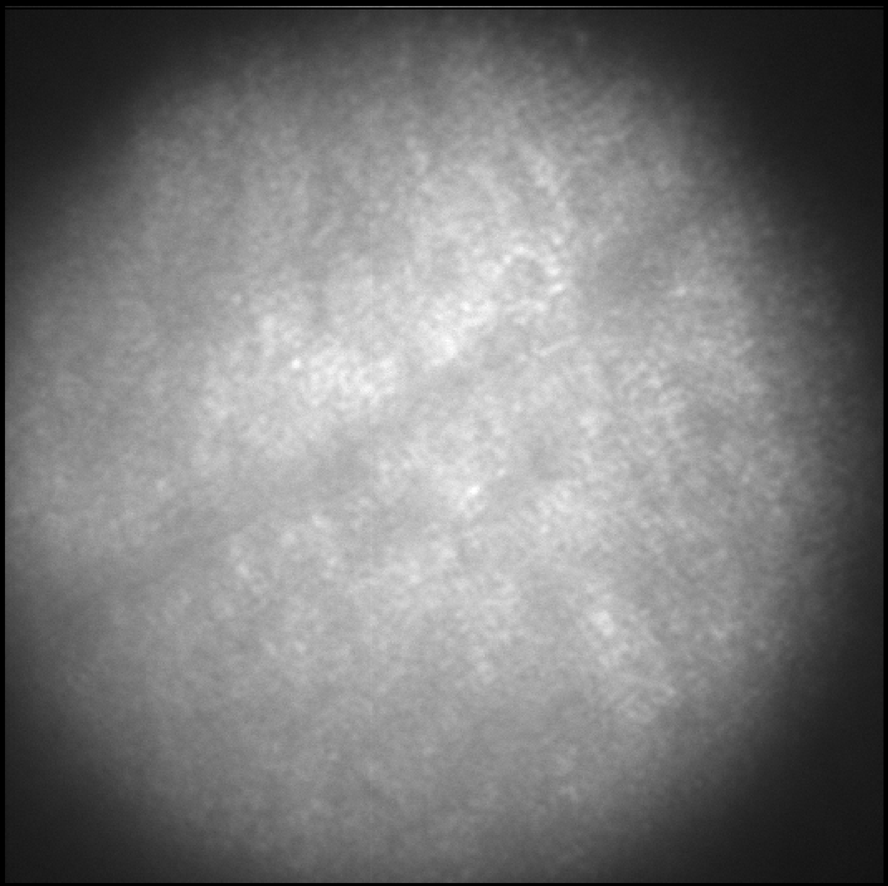

No AO correction

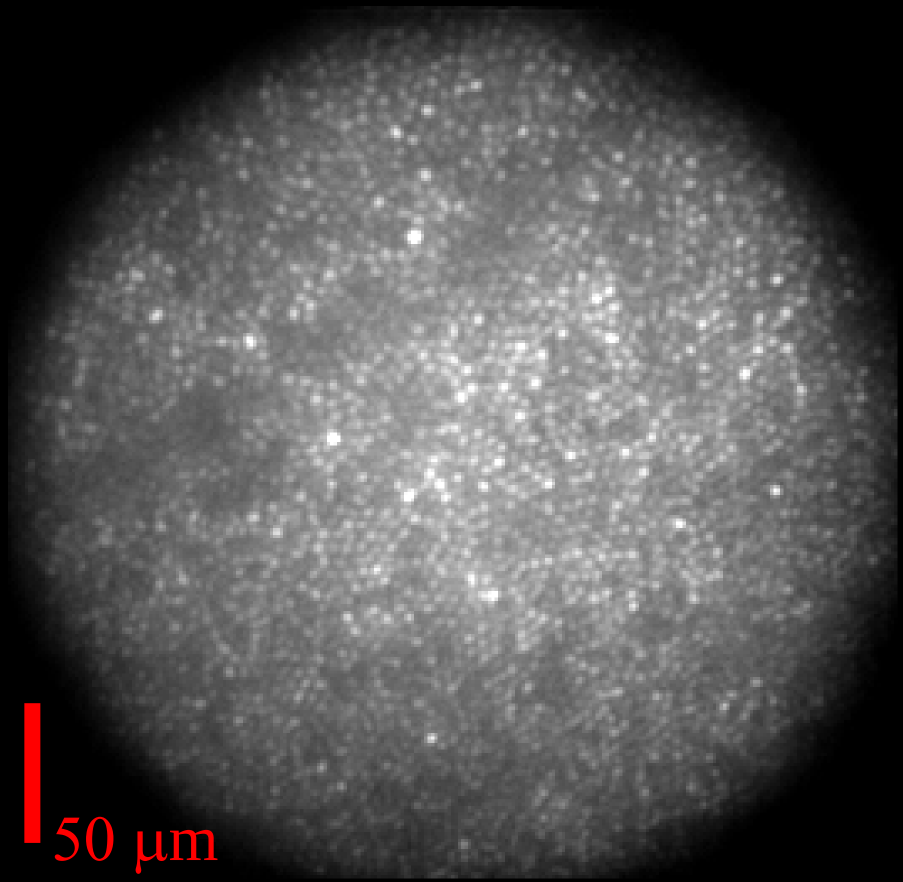


AO correction

**1° field of view; 1.25° eccentricity**

# Through focus video for a fixating eye

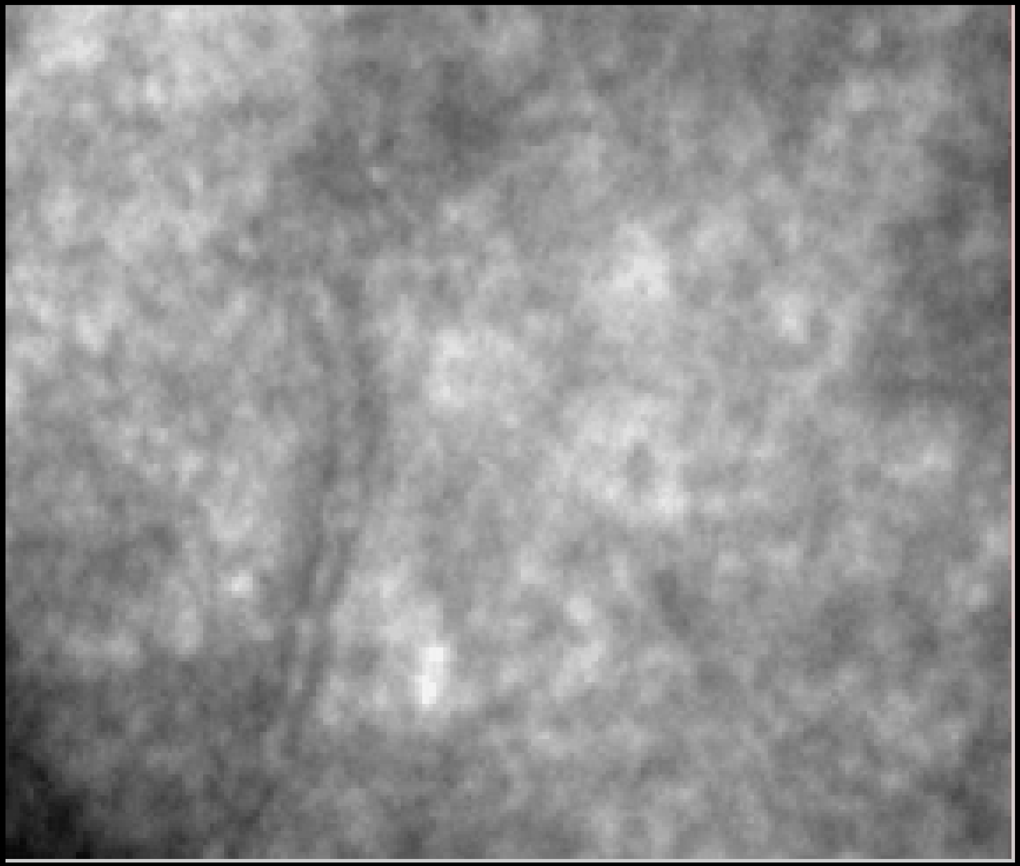

RJ

- Video rate: ~30 fps
- <1° FOV
- 1.25° ecc.
- AO correcting at 22 Hz
- 0.1 μm RMS
- 6 mm pupil

# Blood flow in capillaries: 4-burst imaging

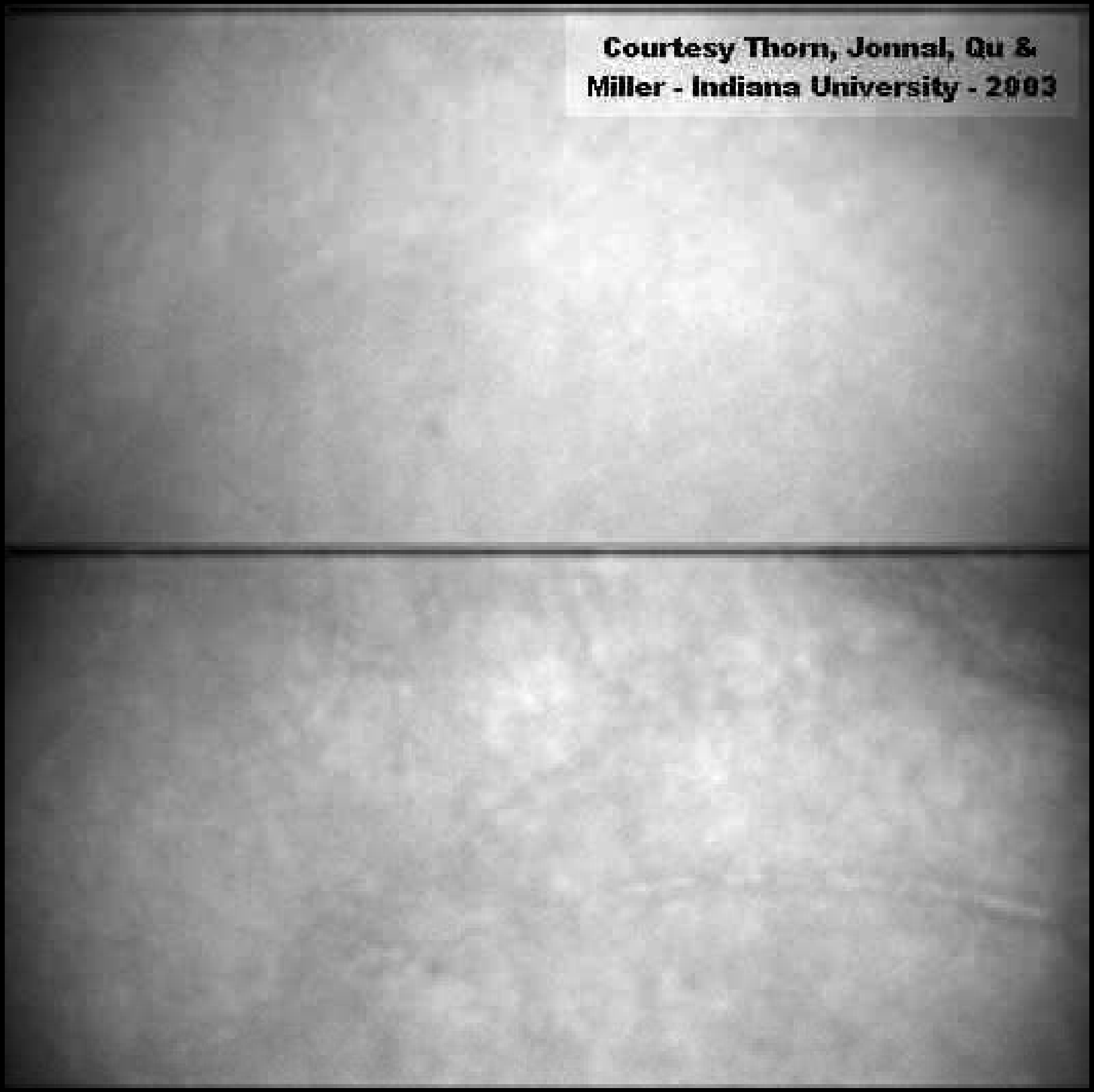


**w/o AO**

1.4 ° retinal ecc.
$\lambda$ = 679 nm
1 msec exp
1 msec delay

Capillary dia
~ 6.6 $\mu$m
Blood velocity
~ 1.5 mm/s

50 $\mu$m

RJ

**w/ AO**

Conventional Retinal Image

# AO-OCT Video of Retinal Cross Section

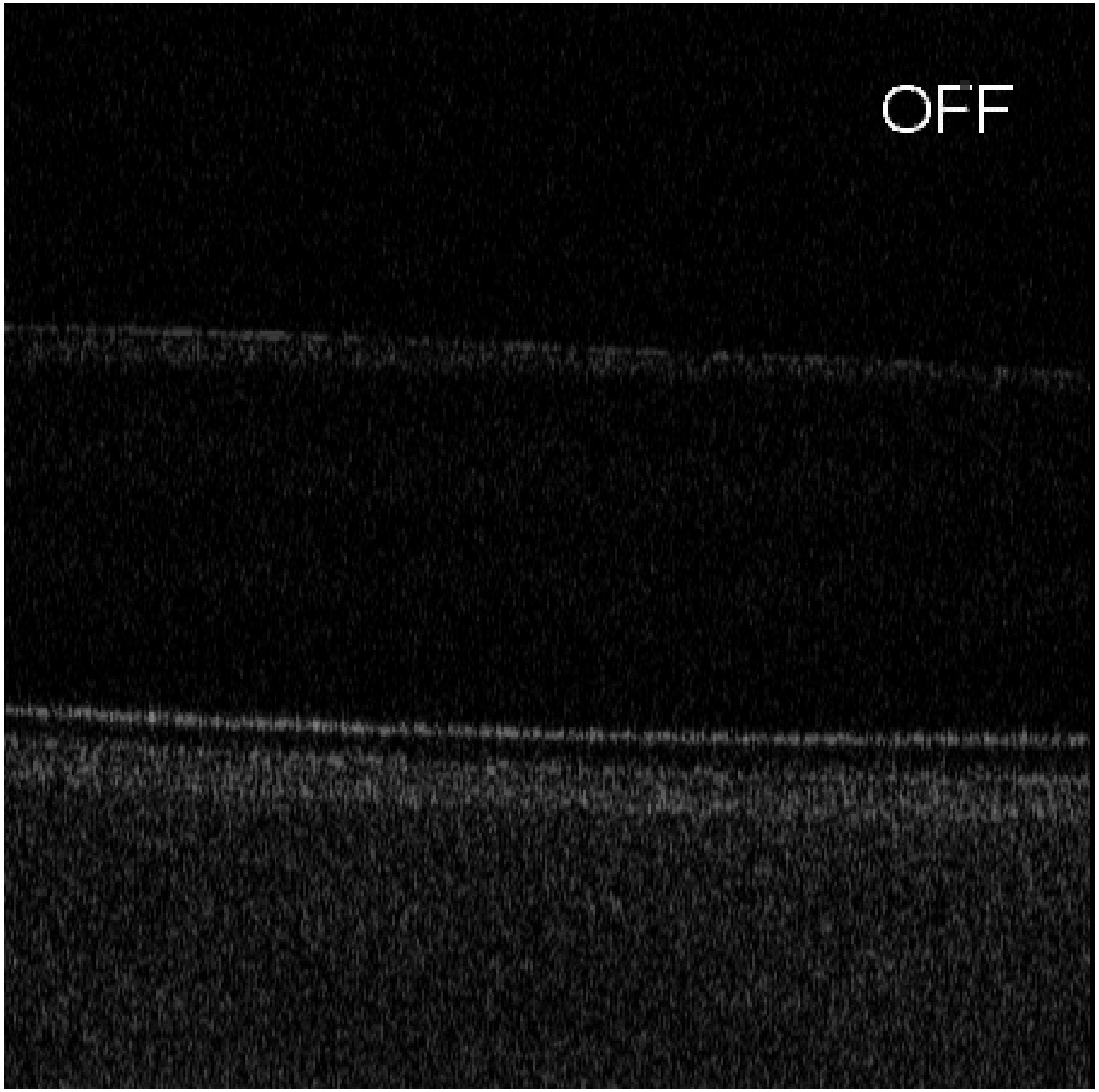


Courtesy R. Zawadski

# Volumetric imaging of retina cells with AO-OCT

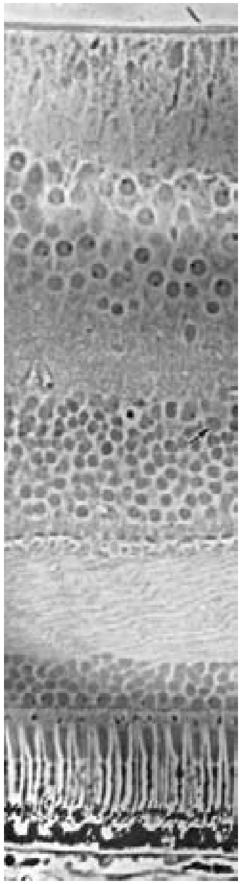

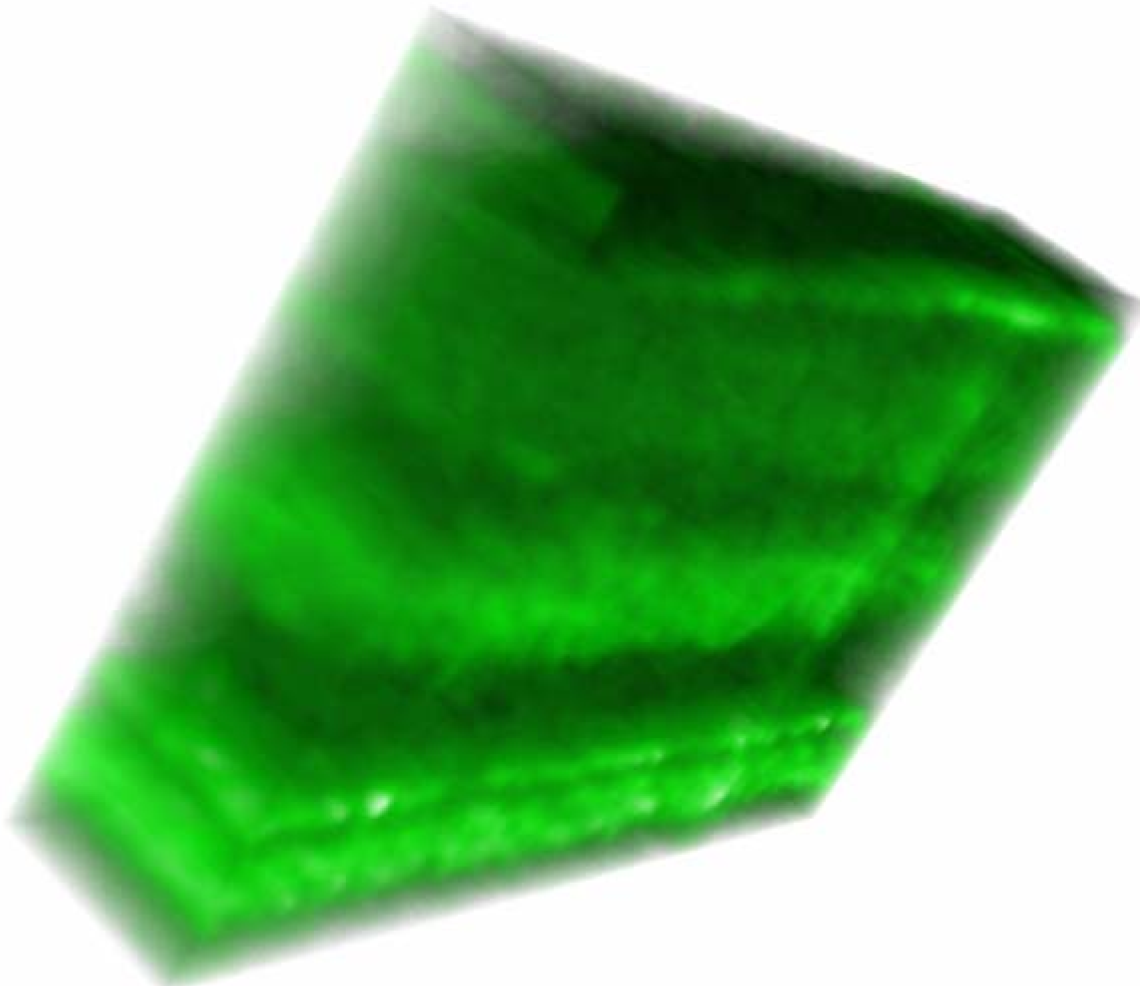

**High 3D resolution and sensitivity permits observation of cone cells in 3 dimensions.**

| GROUP | TYPE | CORRECTOR | PERFORMANCE |
| --- | --- | --- | --- |
| 1. Rochester | Flood<br>cSLO | Xinetics (37,97),<br>BMC (37)<br>BMC (144) | < 0.1 μm RMS, d = 6.8 mm<br>0.12 μm RMS, d = 6 mm<br>Coming Online |
| 2. Houston | cSLO<br>cSLO | Xinetics (37)<br>BMC (144) | 0.15 μm RMS, d = 7 mm |
| 3. Indiana | Flood<br>OCT | Xinetics (37)<br>Xinetics (37),<br>BMC (144) &<br>AOptix (37) | < 0.1–0.2 μm RMS, d=6.8 mm<br>< 0.1–0.2 μm RMS, d=6.8 mm |
| 4. Murcia<br>Murcia &<br>Vienna | Flood<br>OCT | OKO (37),<br>LC-SLM (230,000),<br>OKO (37) | 0.1 μm RMS, d = 5.2 mm<br>~0.1 μm RMS, d = 5.5 mm<br>~0.1 μm RMS, d = 3.68 mm |
| 5. Imperial Col / City, UK | cSLO | OKO (37) | > 0.35 μm RMS, d = 4 mm |
| 6. Galway, Ireland | Flood | OKO (37) | |
| 7. San Diego | Flood | OKO (19) | ~0.3 μm RMS, d = 8 mm |

| GROUP | TYPE | CORRECTOR* | PERFORMANCE |
|---|---|---|---|
| 8. UC Davis / LLNL | Flood OCT | ITEK (109)<br>BMC (144) &<br>Bimorph (37) | ~0.1 μm RMS, d = 7 mm |
| 9. LLNL (will be operated at Doheny) | Phoropter<br>cSLO | BMC (144)<br>BMC (144) and AOptix (37) | Online<br>Online |
| 10. Chengdu, China | Flood | Bimorph (19 or 37) | < 0.2 μm RMS, d = 5 mm |
| 11. Paris | Flood | Bimorph (13) | < 0.3 μm RMS, d = 7 mm |
| 12. Moscow / Kestrel Corp | Flood | Bimorph (18) | > 0.1 μm RMS, d = 4.8 mm |
| 13. Indiana | cSLO | BMC (144) | |

# Summary

1. **Wavefront sensor**
   - SHWS is used exclusively.

2. **Wavefront corrector**
   - many types being used.
   - diffraction limited imaging is very demanding.

3. **Control system**
   -direct slope
   -calibration is critical

4. **Retinal imaging examples**

**AO does work!**